

Variational theory of valence fluctuations: Ground states and quasiparticle excitations of the Anderson lattice model

B. H. Brandow

Theoretical Division, Los Alamos National Laboratory, Los Alamos, New Mexico 87545

(Received 21 January 1985; revised manuscript received 2 December 1985)

A variational study of ground states of the orbitally nondegenerate Anderson lattice model, using a wave function with one variational parameter per Bloch state k , has been extended to deal with essentially metallic systems having a nonintegral number of electrons per site. Quasiparticle excitations are obtained by direct appeal to Landau's original definition for interacting Fermi liquids, $\mathcal{E}_{\text{qp}}(k, \sigma) = \delta E_{\text{total}} / \delta n_{\text{qp}}(k, \sigma)$. This approach provides a simple and explicit realization of the Luttinger picture of a periodic Fermi liquid. A close correspondence is maintained between the "interacting" ($U = \infty$) system and the corresponding "noninteracting" ($U = 0$) case, i.e., ordinary band theory; the result can be described as a renormalized band or renormalized hybridization theory. The occupation-number distribution for the conduction orbitals displays a finite discontinuity at the Fermi surface. If the d - f hybridization is nonzero throughout the Brillouin zone, the quasiparticle spectrum will always exhibit a gap, although this gap becomes exponentially small (i.e., of order T_K) in the Kondo-lattice regime. In the "ionic" case with precisely two electrons per site, such a system may therefore exhibit an insulating (semiconducting) gap. The quasiparticle state density exhibits a prominent spike on each side of the spectral gap, just as in the elementary hybridization model (the $U = 0$ case). For the metallic case, with a nonintegral number of electrons per site, the Fermi level falls within one of the two sharp density peaks. The effective mass at the Fermi surface tends to be very large; enhancements by a factor $\gtrsim 10^2$ are quite feasible. The foregoing variational theory has also been refined by means of a trial wave function having *two* variational parameters per Bloch state k . The above qualitative features are all retained, with some quantitative differences, but there are also some qualitatively new features. The most interesting of these is the appearance, within the Kondo regime, of a significant quasiparticle contribution to the f spectral weight in the vicinity of ϵ_f . The present "one-parameter" and "two-parameter" versions can be viewed as lattice generalizations of the first two approximations of the $(1/N_f)$ -expansion school, although our treatment of lattice aspects departs from strict $1/N_f$ methodology. The two versions have Wilson ratios $\equiv 1$ and $\neq 1$, respectively, consistent with $(1/N_f)$ -expansion studies of the single-impurity model, and a number of other features likewise show good correspondence with $(1/N_f)$ -expansion results. Implications are presented for the finite-temperature behaviors of several properties, especially the specific heat and electrical resistivity. Comparison with experiment then leads to some inferences about the band structures of heavy-fermion materials. A new mechanism is presented for breakup of the coherent Fermi-liquid behavior, as temperature is increased. There are two main approximations: (a) Neglect of the "site exclusion" problem, i.e., within cluster-expansion terms we ignore the requirement that interacting sites must all be distinct. (b) Assumption of a low density of excited quasiparticles (those excited from the "far" side of the hybridization gap) limits the present treatment to very low temperatures, $T \ll T_f$. Electron-number conservation is treated precisely throughout.

I. INTRODUCTION

Fermi-liquid aspects of valence-fluctuation (VF) systems have long been recognized. At first, this connection was based on the Pauli susceptibility and the linear specific heat at low temperatures, and on the similarity of the large effective state densities derived from these two sources. Single-impurity models have generally been employed to describe this level of phenomenology.¹⁻³ Later, the observation of insulating gaps in SmB_6 (Refs. 4 and 5) and TmSe (Ref. 6), and of a sharp Fermi surface in CeSn_3 (Ref. 7), demonstrated that the coherence within a periodic array of "active" sites is very significant. The Luttinger⁸ characterization of a periodic Fermi liquid is therefore particularly relevant here, because this focuses

on features which are sensitive to periodicity and to the number of electrons per site. All Fermi liquids⁹ are characterized by a one-to-one correspondence between their quasiparticle excitation modes and the one-electron excitations of a suitable independent-particle model. The Luttinger picture also includes¹⁰ (1) a Fermi surface defined by a discontinuity in the distribution of conduction-state occupation numbers $n_{k\sigma}$, (2) infinite lifetimes (at $T = 0$) for quasiparticles just on this Fermi surface, and (3) identity between the total number of electrons and the number of quasiparticle states enclosed by the Fermi surface (the Luttinger sum rule). The latter feature strongly suggests an insulating (or semiconducting) gap for those materials where the corresponding independent-particle model (ordinary band theory) has such a gap. The important conclusion that the Luttinger picture applies to VF

materials is due to Martin and Allen.¹¹

In recent years, remarkable progress has been achieved on single-impurity models, both via exact “benchmark” results from the renormalization group¹² and Bethe ansatz^{13–16} methods, and via reasonably simple yet accurate approximations based on the “(1/ N_f)-expansion” idea.^{17–24} ($N_f = 2J + 1$ is the effective ionic-ground-state degeneracy.) The latter approach offers the prospect of extending the single-impurity results to more realistic systems for which the exact results do not apply. Unfortunately, however, it has appeared that a strict $1/N_f$ expansion would describe a lattice as built up from a single-impurity term ($\sim N_f^0$), followed by a two-impurity term ($\sim N_f^{-1}$), a three-impurity term ($\sim N_f^{-2}$), etc.^{25–28} It seems very unlikely that such an approach can ever adequately explain the specifically periodic features (Fermi surface and insulating gap), since these features are probably associated with asymptotically high orders of the multisite expansion. To be practical, a treatment of the periodic features must therefore sum the entire multisite expansion and deal with this in a closed form.²⁹ Thus, a different approach to the lattice problem should be sought.

Previous work on the lattice problem has included a variety of Green’s-function treatments,^{30–37} functional integration,^{27,38,39} real-space renormalization group,^{40–42} perturbation expansion in U ,⁴³ and the variational method.^{30(b),44–47} However,, none of these efforts have provided an adequate treatment of *both* the insulating gap and Fermi-surface aspects.^{48,49}

We have now found a viable treatment of the periodic aspects, by elaborating a previous variational approach^{30(b),45} for ground states of Anderson lattice systems. Actually, two different levels of approximation have been developed. The first, the “one-parameter” version, has one variational parameter per Bloch state k . Its algebra is so simple and transparent that a number of useful results can be obtained analytically. The second approximation, the “two-parameter” version, has two variational parameters per Bloch k . This should be more accurate, and it introduces some qualitatively new features, but the algebra is now tedious and numerical methods are required throughout. Nevertheless, even for the latter version the mathematical apparatus is simple enough that inclusion of a number of the complex details of real systems (orbital degeneracy, spin-orbit coupling, crystal-field splitting, band structure, etc., as well as finite temperature) should be feasible.

A close correspondence between these two versions and the first two stages of the $1/N_f$ expansion is immediately evident, although our treatment of the lattice aspect does not follow $1/N_f$ methodology. The lattice features and the Fermi-liquid features are incorporated in a transparent manner from the outset. The result (in either version) is an explicit realization of the Luttinger picture of a periodic Fermi liquid. A one-to-one connection between the strong-interaction ($U = \infty$) results and the simple $U = 0$ case (ordinary band theory) is clearly displayed. The overall result can, therefore, also be characterized as a “renormalized band” or “renormalized hybridization” theory.

We do not claim to have proven that the Luttinger (periodic Fermi liquid) description is correct for these systems. Indeed, Luttinger⁸ has commented that the only unassailable proof would be an exact solution. In common with most of the other theoretical literature on Fermi-liquid systems, we merely *assume* that this description is correct, and then proceed to work out the consequences. In practical terms, the important question is whether some other type of phase could have a lower free energy; the main competitors here are an ordinary magnetic phase [with moments at least partially unquenched, and Ruderman-Kittel-Kasuya-Yosida (RKKY) coupling],^{38,40,41,50} and a superconducting phase. We have not pursued this issue. The justification for the present work must rest on the results obtained, namely, the overall consistency with (exact) single-impurity results, and also the similarity to known experimental behaviors.

The purpose of this paper is to provide an introduction and overview, i.e., to present the basic concepts and some illustrative results, without getting into much technical detail. A key feature of the method is diagrammatic analysis. This is based on a many-body (linked cluster) perturbative formalism developed originally for problems in nuclear⁵¹ and atomic and molecular physics,⁵² and still generally unfamiliar to the solid-state physics community.⁵³ Also, our more refined variational approximation involves considerable algebra. We therefore begin by emphasizing the simple features and main results, postponing these details for later publications.

We use the following form of Anderson lattice Hamiltonian,

$$H = \sum_{k,\sigma} \epsilon_k \hat{n}_{k\sigma} + \epsilon_f \sum_{j,\sigma} \hat{n}_{j\sigma} + U \sum_j (1 - \hat{n}_{j\uparrow})(1 - \hat{n}_{j\downarrow}) + \sum_{k,j,\sigma} (v_{kj} \eta_{k\sigma}^\dagger \eta_{j\sigma} + \text{H.c.}), \quad (1)$$

where j is a site index. U is taken to be infinite. Orbital degeneracy is ignored, as well as any intrinsic f -electron bandwidth. The use of $(1 - \hat{n}_{j\uparrow})(1 - \hat{n}_{j\downarrow})$ rather than $\hat{n}_{j\uparrow}\hat{n}_{j\downarrow}$, in the Hubbard term, means that fluctuation takes place between f^1 and f^2 configurations, instead of f^0, f^1 . This form is more appropriate for Sm and Yb materials, and, more importantly, it makes the diagrammatic analysis more transparent. Results for the more familiar form of H (with $\hat{n}_{j\uparrow}\hat{n}_{j\downarrow}$) can easily be deduced, since these two forms are simply related by particle-hole transformation.

In all of the numerical results presented we use the following Hamiltonian parameters: $W = 2$ eV, the bandwidth of the bare (ϵ_k) conduction states, with a constant (rectangular) density of states, and $V = -(0.05)^{1/2}$ eV, the (k -independent) strength of the df hybridization in Bloch representation,

$$V_k = N^{-1/2} \sum_j e^{ik \cdot R_j} v_{kj} \rightarrow V, \quad (2)$$

where N is the number of sites. The origin of the energy scale is at ϵ_f , i.e., $\epsilon_f \equiv 0$, and the conduction-band limits are D_+ and $-D_-$ for the top and bottom, respectively ($D_+ + D_- = W$; $D_- > 0$ means ϵ_f above bottom of band). Also, all cases shown have 2.4 electrons per site, making

them intrinsically metallic as appropriate for intermetallic compounds. Extension to the ionic (and possibly insulating) case, with just 2 electrons per site, will be obvious. The use of a nonintegral electron number per site, 2.4, may be viewed as a proxy for a somewhat more realistic model with a five-fold degenerate “5d” conduction band, and 4 electrons per site.

To emphasize the connections with the noninteracting ($U=0$) case, i.e., the Luttinger aspects, we shall discuss three cases: The $U=0$ case (in Sec. II), the interacting ($U=\infty$) case with one variational parameter per Bloch state k (Secs. III and IV), and the $U=\infty$ case with two variational parameters per k state (Sec. V). Extensive discussion is presented in Sec. VI, followed by concluding remarks in Sec. VII. The discussion includes (a) implications for low-temperature phenomenology (specific heat, magnetic susceptibility, and electrical transport properties), (b) comparisons with previous single-impurity results, and (c) present simplifications and approximations that deserve further effort. A brief report of this work has been presented previously.⁵⁴

II. THE $U=0$ CASE

The noninteracting ($U=0$) case is just the elementary problem of hybridization between two bands, one of which has zero width. The result is shown in Fig. 1, for $D_- = 1.3$ eV. For each k there are two hybridized or “quasiparticle” states, with energies

$$\mathcal{E}_k^\pm = \frac{1}{2} \{ \epsilon_k + \epsilon_f \pm [(\epsilon_k - \epsilon_f)^2 + 4V_k^2]^{1/2} \}. \quad (3)$$

There is a small gap, whose width Δ is, by second-order perturbation theory,

$$\Delta \approx \frac{V^2}{D_-} + \frac{V^2}{D_+}. \quad (4)$$

If there were just 2 electrons per site, the Fermi level

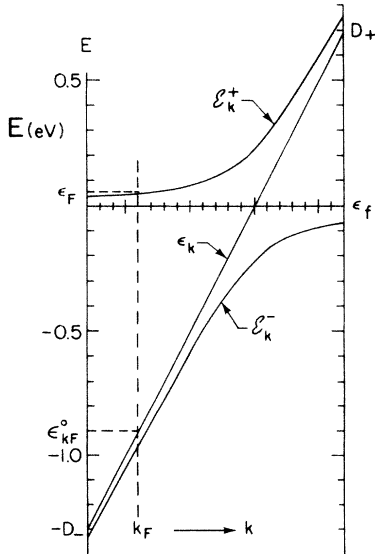


FIG. 1. Quasiparticle spectrum for $U=0$ case. Input parameters are $W=2.0$ eV, $V=-(0.5)^{1/2}$ eV, $D_- = 1.3$ eV, $\epsilon_{kF}^0 = -0.9$ eV.

would obviously fall in this gap and produce an insulating (semiconducting) state. With 2.4 electrons, however, the Fermi level ϵ_F falls in the upper (\mathcal{E}^+) quasiparticle band. [Note the distinction between ϵ_F and ϵ_{kF}^0 in Fig. 1, where $\epsilon_{kF}^0 \equiv \epsilon_k(k=k_F)$.] The band is quite flat near this ϵ_F , corresponding to a large effective mass (in this case, enhancement by factor of $19.1 \equiv m^*$, as compared to the “bare” ϵ_k spectrum). As is intuitively obvious, the f -electron content of a quasiparticle is largest where the band is most flat. This will be shown in more detail in Sec. IV.

We note, for comparison below, that this case can be viewed as a variational problem based on the trial wave function

$$\Psi = \left[\prod_{j,\sigma} \left[1 + \sum_k a_{kj} \eta_{k\sigma}^\dagger \eta_{j\sigma} \right] \right] | \Phi_c \Phi_f \rangle, \quad (5)$$

where

$$\Phi_f = \left[\prod_j \eta_{j\uparrow}^\dagger \eta_{j\downarrow}^\dagger \right] | \text{vacuum} \rangle \quad (6)$$

shows all $2N$ localized “ f ” orbitals initially occupied, and Φ_c is a simple Fermi sea containing $0.4N$ conduction electrons. In Bloch representation this becomes

$$\Psi = \left[\prod_{k>,\sigma} (1 + A_k \eta_{k\sigma}^\dagger \eta_{fk\sigma}) \right] | \Phi_c \Phi_f \rangle, \quad (7)$$

$$\Phi_f = \left[\prod_k \eta_{fk\uparrow}^\dagger \eta_{fk\downarrow}^\dagger \right] | \text{vacuum} \rangle, \quad (8)$$

$$A_k = N^{-1/2} \sum_j e^{ik \cdot R_j} a_{kj}. \quad (9)$$

(Throughout this paper we use $k_>, k_<$ to denote the states $k \gtrless k_F$, or more correctly, $\epsilon_k \gtrless \epsilon_{kF}^0$.)

This variational problem decomposes into a “direct product” of elementary problems, one for each state $k\sigma$. The energy expectation value is easily seen to be

$$\langle H \rangle = \sum_{k<,\sigma} \epsilon_k + \sum_{k>,\sigma} \frac{\epsilon_k A_k^2 + 2V_k A_k}{1 + A_k^2}, \quad (10)$$

thus the optimization condition is

$$\frac{\delta \langle H \rangle}{\delta A_k} = \frac{4}{(1 + A_k^2)^2} (\epsilon_k A_k + V_k - V_k A_k^2) = 0, \quad (11)$$

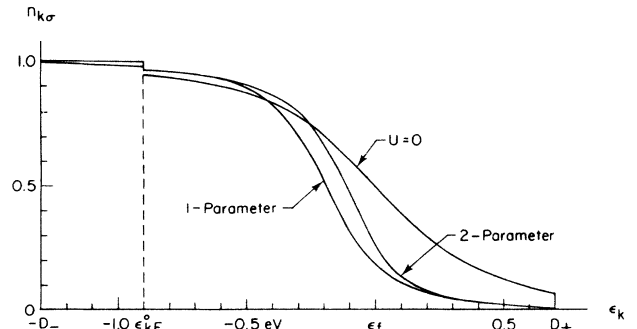


FIG. 2. Conduction-state occupation-number distributions. Same input as Fig. 1.

and

$$A_k = \frac{1}{2} \left\{ \frac{\varepsilon_k}{V_k} + \left[\left(\frac{\varepsilon_k}{V_k} \right)^2 + 4 \right]^{1/2} \right\}. \quad (12)$$

The occupation numbers for the conduction states are

$$n_{k\sigma} = A_k^2 / (1 + A_k^2) \quad (13)$$

for $k > k_F$, and unity for $k < k_F$, as shown in Fig. 2.

III. ONE-PARAMETER THEORY

For the interacting ($U = \infty$) case, our "one-parameter" trial wave function is⁵⁵

$$\Psi = \left[\prod_j \left(1 + \sum_{k,\sigma} a_{kj} \eta_{k\sigma}^\dagger \eta_{j\sigma} \right) \right] | \Phi_c \Phi_f \rangle. \quad (14)$$

Note that this form of Ψ prohibits any f^0 configurations, and it also conserves electron number. After transforming to Bloch representation, there is seen to be just one free parameter, A_k , for each Bloch state k . This statement involves the assumption of complete site equivalence,⁵⁶ whereby

$$a_{kj} = N^{-1/2} A_k e^{-ik \cdot R_j}. \quad (15)$$

Some prominent features of valence-fluctuation materials follow almost immediately from this form of Ψ .^{30(b),45} For example, the only way to admix magnetic configurations ($\eta_{j\sigma}$) with the nonmagnetic initial configuration ($| \Phi_c \Phi_f \rangle$), and gain ground-state binding energy by doing so, is to have the magnetic configurations coupled with conduction electrons ($\eta_{k\sigma}$) so as to form a singlet. This explains why the magnetic moments of most VF materials are quenched at low temperatures. Another important qualitative feature is discussed below, following Eq. (23).

By an approximate diagrammatic analysis (see discussion in Sec. VI G) we obtain the conduction-state occupation numbers

$$n_{k\sigma} = \begin{cases} 1, & k < k_F \\ A_k^2 / (\mathcal{D} + A_k^2), & k > k_F \end{cases} \quad (16)$$

[compare with (13)], and the total-energy expectation value,

$$\langle H \rangle = \sum_{k < \sigma} \varepsilon_k + \sum_{k > \sigma} \frac{\varepsilon_k A_k^2 + 2V_k A_k}{\mathcal{D} + A_k^2} \quad (17)$$

[compare with (10)], where \mathcal{D} plays the role of a one-site normalization factor. Actually,

$$\frac{1}{\mathcal{D}} = 1 - \frac{1}{N} \sum_{k > \sigma} \frac{A_k^2}{\mathcal{D} + A_k^2} = \langle \hat{n}_j \hat{n}_{j_1} \rangle = 1 - \xi \quad (18)$$

is the true probability of f^2 configurations. The parameter ξ , the probability of f^1 configurations, is our measure of the average valence. It follows, then, from these configuration probabilities, that

$$\begin{aligned} n_{j\sigma} &= P(f^2) + \frac{1}{2} P(f^1) = (1 - \xi) + \frac{1}{2} \xi \\ &= 1 - \frac{1}{2} \xi. \end{aligned} \quad (19)$$

The results (16)–(18) are so simple that the diagrammatic analysis is not really essential here; they can also be obtained directly by a simple intuitive argument.^{30(b),45} In this approximation, the various sites j interact *only* via the exclusion principle, namely, the fact that two sites cannot simultaneously make use of the same Bloch orbital $k\sigma$. Thus, if site j has made the (virtual) transition $j\uparrow \rightarrow k\uparrow$, then the corresponding transition $j'\uparrow \rightarrow k\uparrow$ is blocked (momentarily forbidden) for all of the other sites $j' \neq j$. It follows that the $k\sigma$ orbital occupation number can be evaluated as a sum of quasi-independent one-site contributions

$$n_{k\sigma} = \sum_j \frac{|a_{kj}|^2}{\mathcal{D}} \left[1 - \frac{N-1}{N} n_{k\sigma} \right], \quad (20)$$

where $1 - (N-1)n_{k\sigma}/N$ represents the probability that $k\sigma$ is not already occupied by an electron from some other site $j' \neq j$. Thus, $n_{k\sigma}$ is the product of an "attempt probability," $\mathcal{D}^{-1} \sum_j |a_{kj}|^2$, and a "success probability" or blocking factor, $[1 - (N-1)n_{k\sigma}/N]$. For large N this simplifies to

$$n_{k\sigma} = (A_k^2 / \mathcal{D})(1 - n_{k\sigma}) = A_k^2 / (\mathcal{D} + A_k^2), \quad (21)$$

in view of (15). Similarly, the normalization denominator is

$$\mathcal{D} = 1 + \sum_{k > \sigma} |a_{kj}|^2 (1 - n_{k\sigma}) = 1 + \frac{1}{N} \sum_{k > \sigma} \frac{A_k^2 \mathcal{D}}{\mathcal{D} + A_k^2}. \quad (22)$$

Note that the states $k < k_F$ do not contribute here. They are effectively inert because they are already fully occupied, from Φ_c . When (22) is reexpressed in the form (18), the last equality (which gives ξ as a function of the A_k 's) follows as a direct consequence of electron-number conservation. The derivation of the $\langle H \rangle$ expression (17) is completed by associating a blocking factor $(1 - n_{k\sigma})$ with each of the hybridization terms, thus

$$\langle v \rangle = \sum_{k > j, \sigma} (v_{jk} a_{kj} + \text{H.c.})(1 - n_{k\sigma}). \quad (23)$$

It will be shown in a future paper that the diagrams we retain and sum have precisely the physical interpretation just given.

This elementary argument has the virtue of demonstrating that the dominant interaction between the active sites (the exclusion-principle blocking effect) is effectively a *destructive interference*. The destructive or repulsive character of this interaction serves to explain why there is no collective phase transition in most VF materials, as they are cooled to low temperatures. We consider this result to be an essential ingredient (together with the arguments for Fermi-liquid behavior of a single impurity⁵⁷) for understanding why the paramagnetic Fermi-liquid picture applies to most VF materials, or in other words, why there is generally no order parameter.

The optimization condition is now a bit more complicated than in Sec. II,

$$\frac{\delta\langle H \rangle}{\delta A_k} = \frac{\partial\langle H \rangle}{\partial A_k} + \frac{\partial\langle H \rangle}{\partial \mathcal{D}} \frac{\delta \mathcal{D}}{\delta A_k}$$

$$= \frac{4V_k}{(\mathcal{D} + A_n^2)^2} \left\{ \mathcal{D} \left[A_k \left(\frac{\epsilon_k - \mu}{V_k} \right) + 1 \right] - A_k^2 \right\} = 0, \quad (24)$$

where μ , a ‘‘pseudo chemical potential,’’ arises from the dependence of \mathcal{D} upon A_k . (Details concerning the μ parameter are presented in the Appendix.) It is convenient to express the solution as

$$A_k = \mathcal{D}^{1/2} [y_k + (y_k^2 + 1)^{1/2}] \equiv \mathcal{D}^{1/2} \hat{A}_k, \quad (25)$$

where

$$y_k = \mathcal{D}^{1/2} (\epsilon_k - \mu) / 2V_k. \quad (26)$$

Using $\mathcal{D} = (1 - \xi)^{-1}$, we see that the ‘‘basic parameters,’’ which characterize the A_k and $n_{k\sigma}$ distributions, can be chosen as ξ and μ . Both of these involve integrations over k (subject to $k > k_F$) of functions of A_k , and are therefore themselves functions of ξ and μ . With constant density of states ($\rho_0^\sigma = W^{-1}$) and constant V ($V_k \rightarrow V$) the integrals are elementary, and we then have two equations to solve numerically. These equations are

$$\xi = \frac{1}{N} \sum_{k>\sigma} \frac{A_k^2}{\mathcal{D} + A_k^2} = \frac{2|V|}{W\mathcal{D}^{1/2}} (\hat{A}_- - \hat{A}_+), \quad (27)$$

$$\mu = \frac{\mathcal{D}}{N} \sum_{k>\sigma} \frac{V_k A_k}{\mathcal{D} + A_k^2} = -\frac{2V^2}{W} [\ln(\hat{A}_- / \hat{A}_+)]. \quad (28)$$

The subscript $+$ ($-$) represents the value of \hat{A} at the top (bottom) of the initially empty part of the conduction band, corresponding to $\epsilon_k = D_+$ ($\epsilon_k = \epsilon_{kF}^0$). [Observe that $y_- > y_+$ and $\hat{A}_- > \hat{A}_+ > 0$, because we are assuming $V < 0$. The latter is convenient because, in order that the hybridization energy (23) be attractive, A_k must then be positive.] The resulting ξ and μ are shown in Fig. 3, as functions of D_- . From comparison of (28) with (23) and (21), we note that

$$\mu = \langle v \rangle / 2N.$$

This result facilitates comparison with other formalisms.⁴⁹ For completeness, we also note (see Appendix) that

$$\frac{\langle H \rangle}{N} = \sum_{k<\sigma} \epsilon_k + \mu - \frac{2V^2}{W} (1 - \xi)(y_- \hat{A}_- - y_+ \hat{A}_+). \quad (29)$$

Before discussing ground-state properties, we note that there are three different regimes to consider.⁴⁵ When ϵ_f lies below the bottom of the initially empty part of the conduction band ($\epsilon_f < \epsilon_{kF}^0$, or $D_- < 0.4$ eV here), only ‘‘virtual’’ transitions $j\sigma \rightarrow k_>\sigma$ are possible. These transitions are well described by perturbation to second order in V (provided $\epsilon_{kF}^0 - \epsilon_f \geq |V|$), hence we call this the perturbative regime. The probability of simultaneous $j\uparrow \rightarrow k_>\uparrow$ and $j\downarrow \rightarrow k_>\downarrow$ transitions is inherently so small

here that U should have little effect. When ϵ_f lies above ϵ_{kF}^0 there is an obvious tendency for electrons to vacate some of the f orbitals and fall into conduction orbitals with $\epsilon_{kF}^0 < \epsilon_k < \epsilon_f$. If V were absent, such $f \rightarrow d$ transfers would continue until either the conduction-state Fermi level rises to meet ϵ_f or until one electron has been removed from each of the f sites and U will then not permit any further transfers. The former case ($\epsilon_{kF}^0 < \epsilon_f < \epsilon_{kF}^0 + \frac{1}{2}W$, or $0.4 < D_- < 1.4$ eV) defines the valence-fluctuation or mixed-valent regime, and the latter case ($\epsilon_f > \epsilon_{kF}^0 + \frac{1}{2}W$, or $D_- > 1.4$ eV) defines the Kondo-lattice regime. These regimes are indicated at the bottom of Fig. 3.

The V -interaction energy ($\langle H \rangle / N$ minus corresponding energy for $V=0$) is shown as a function of D_- in Fig. 3. Note the strongly contrasting behaviors in the three regimes, and the smooth crossovers between these regimes. In the perturbative regime $\langle H \rangle_{\text{int}} / N$ agrees with second-order perturbation in V , falling asymptotically as $|D_- - 0.4 \text{ eV}|^{-1}$. ξ and μ are both small, as expected. In the VF regime $\langle H \rangle_{\text{int}} / N$ reaches its maximum but still varies rather slowly with D_- , while ξ varies linearly with D_- . (Compare with ξ_0 in Fig. 3, which shows the behavior of ξ for the case $V=0$, $U=\infty$.) In the Kondo-lattice regime, however, $\langle H \rangle_{\text{int}} / N$ shows a rapid exponential falloff with increasing D_- ,

$$N^{-1} \langle H \rangle_{\text{int}} \approx -D_K \exp[-(\epsilon_f - \hat{\epsilon}_F)W / 2V^2], \quad (30)$$

where $\hat{\epsilon}_F \equiv \epsilon_{kF}^0 + \frac{1}{2}W$ is the Fermi level for the corresponding $V=0$, $U=\infty$ system, and $D_K = D_+ - \hat{\epsilon}_F$ is the energy difference between the top of the band and $\hat{\epsilon}_F$. (The inclusion of ϵ_f in the exponent is only for the sake of clarity, since we are using $\epsilon_f \equiv 0$. Note also that D_K depends on electron number, i.e., on ϵ_{kF}^0 , but not on the position of ϵ_f .) Also $1 - \xi$ varies with the same rapid exponential factor,

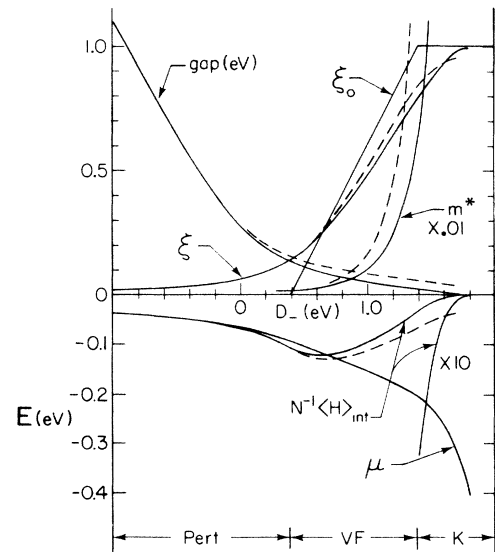


FIG. 3. Results of one-parameter and two-parameter models: solid and dashed lines, respectively. ξ_0 is valence parameter for $V=0$, $U=\infty$. Same input as Fig. 1. Note the three different regimes, shown at bottom.

$$1 - \xi \approx \frac{W}{2V^2} \left| \frac{1}{N} \langle H \rangle_{\text{int}} \right|, \quad (31)$$

whereas

$$\mu \approx -(\varepsilon_f - \hat{\varepsilon}_F) - \frac{1}{2} W(1 - \xi). \quad (32)$$

Note from Fig. 3 that $0 < \xi < 1$ and $\mu < 0$ hold everywhere. In general, μ is small (of order V^2/W) until reaching the Kondo regime, where it quickly approaches $-(\varepsilon_f - \hat{\varepsilon}_F)$. A moment's reflection shows that this μ behavior is necessary for electron-number conservation, since $\varepsilon_k = \mu$ defines the point at which $n_{k\sigma} = \frac{1}{2}$. We see from (18) and (26) that V_k is effectively renormalized down to $V_k(1 - \xi)^{1/2}$, thus the $n_{k\sigma}$ distribution is both sharpened (by $1 - \xi$) and shifted downwards in energy (by μ), as shown in Fig. 2. These effects are most dramatic in the Kondo regime, where the $n_{k\sigma}$ distribution rapidly approaches the form of a step function, with the jump pinned at $\hat{\varepsilon}_F$. In this case the system *appears* to have *two* Fermi levels: the *true* one at $\varepsilon_k = \varepsilon_{kF}^0$, with a very small but finite jump in $n_{k\sigma}$, and a "pseudo Fermi level" at $\varepsilon_k = \mu \approx \hat{\varepsilon}_F$, where naive ($V=0$) arguments would place ε_F , with $n_{k\sigma}$ actually continuous here but falling very rapidly.

For all three regimes, the above qualitative features can all be obtained analytically, from (27)–(29), by exploiting the asymptotic approximations

$$\hat{A} = y + (y^2 + 1)^{1/2} \rightarrow \begin{cases} 2y + (2y)^{-1}, & y \gg 1 \\ (2|y|)^{-1}, & y \ll -1. \end{cases} \quad (33)$$

These approximations have a wide range of validity, because $|V|/W$ is generally quite small. They fail to apply only in the crossover regimes, where either $|y_-| \lesssim 1$ or $|y_+| \lesssim 1$. This is the motivation for expressions (25) and (26). The analytical behaviors in the various regimes will be discussed more fully in a future paper.

IV. QUASIPARTICLE SPECTRA AND STATE DENSITIES

To obtain the quasiparticle or elementary-excitation energies, we appeal directly to the original Fermi-liquid concept,⁹ namely, the idea of a one-to-one correspondence between the interacting ($U = \infty$) and noninteracting ($U = 0$) systems. For the ground state we obviously have

$$\Psi_g = \Omega \Phi_0, \quad (34)$$

where Ψ_g represents the "true" (actually variational) ground state, $\Phi_0 = |\Phi_c \Phi_f\rangle$ is the noninteracting reference state, and the "wave operator" Ω is just a shorthand notation for the correlations and all of the details of our calculational procedure. We simply assume, now, that this relation continues to hold for the elementary excited states. Suppose we add one $k\uparrow$ quasiparticle to the system, with $k > k_F$. We add the bare conduction electron $k\uparrow$ to Φ_c , and use the same recipe for Ω as before. Examining the equations for $\langle H \rangle$, \mathcal{D} , ξ , and μ , namely (17), (18), (27), and (28), we see that this $k\uparrow$ state is now to be treated "as if" it were below k_F . In other words, this $k\uparrow$ is now to be *added* to the $k_<, \sigma$ sums in these expressions, and *re-*

moved from their $k_>, \sigma$ sums. Fortunately, however, it is not necessary to resolve the equations for ξ and μ , because $\langle H \rangle$ is stationary with respect to small [here $\mathcal{O}(N^{-1})$] changes in the A_k 's. The net change in total energy is therefore

$$\mathcal{E}_k^+ = \varepsilon_k - \frac{\varepsilon_k A_k^2 + 2V_k A_k}{\mathcal{D} + A_k^2} + \frac{\mu A_k^2}{\mathcal{D} + A_k^2}. \quad (35)$$

The first two terms come from the obvious changes in $\langle H \rangle$ [see (17)], while the last term comes from the corresponding change in \mathcal{D} , $(\partial \langle H \rangle / \partial \mathcal{D}) \delta \mathcal{D}$. Using (24), the stationary condition for A_k , this simplifies to

$$\mathcal{E}_k^+ = \varepsilon_k - \frac{V_k A_k}{\mathcal{D}}. \quad (36)$$

Details are given in the Appendix. Now consider *removing* one of the $k < k_F$ states from Φ_c (with $\sigma = \uparrow$, say), thereby changing its status from " $k_< \uparrow$ " to " $k_> \uparrow$." We find the same expression for the quasiparticle energy. We now have the full spectrum for the *upper* (\mathcal{E}^+) quasiparticle band.

In effect, we are employing the original Landau definition⁹ of the quasiparticle energies,

$$\mathcal{E}_{\text{qp}}(k, \sigma) = \frac{\delta E_{\text{total}}}{\delta n_{\text{qp}}(k, \sigma)}, \quad (37)$$

where $n_{\text{qp}}(k, \sigma)$ is the "quasiparticle occupation number" for state $k\sigma$. We implement this formal definition by identifying the n_{qp} 's with the orbital occupation numbers for the Φ_0 of (34). It is obvious, from the present construction, that each quasiparticle contains exactly one electron, i.e., addition (removal) of a quasiparticle must raise (lower) the total electron number by unity.

The energies of the *lower* (\mathcal{E}^-) subband require a more subtle analysis. We consider the Bloch representation for Φ_f , Eq. (8), and *remove* an $fk\uparrow$ state, assuming for now that $k > k_F$. By momentum conservation, this operation is seen to delete $k\uparrow$ from the $k_>, \sigma$ sums in $\langle H \rangle$ and \mathcal{D} , thereby giving the second and third terms of Eq. (35). But there is now a further effect to consider. Within both \mathcal{D} and $\langle H \rangle$, the virtual transitions $j\sigma \rightarrow k'\sigma$ are allowed *only* when $j\uparrow$ and $j\downarrow$ are *both* initially occupied. Removal of $fk\uparrow$ has left the $j\uparrow$ of Φ_f unoccupied by the fractional amount N^{-1} , and therefore all virtual $j\sigma \rightarrow k'\sigma$ processes are suppressed by this amount. The consequences are analyzed in the Appendix. The net result is to shift all of the \mathcal{E}_k^- energies downwards by the amount μ (recall $\mu < 0$), thus

$$\mathcal{E}_k^- = \frac{V_k A_k}{\mathcal{D}} + \mu. \quad (38)$$

By continuity, we find the same result for $k < k_F$.

By direct substitution, using (25) and (26), one finds that the resulting spectra have exactly the same form (3) as in the elementary hybridization model, but with renormalized parameters,

$$\varepsilon_f \rightarrow \tilde{\varepsilon}_f = \varepsilon_f + \mu, \quad (39)$$

$$V_k \rightarrow \tilde{V}_k = V_k(1 - \xi)^{1/2}. \quad (40)$$

The resulting “renormalized-band” or “renormalized-hybridization” aspect is discussed further below and in Sec. VI.

It follows that there is a spectral gap similar to that of the $U=0$ case, Eq. (4), but *reduced*, now, by the factor $1-\xi$. This reduction of gap width is most significant in the Kondo regime. The location of the gap is shifted downwards by μ . In the Kondo regime, (32) shows that this places the gap near $\hat{\epsilon}_F$, a finite distance below ϵ_f . The *outer* band limits (top of \mathcal{E}^+ and bottom of \mathcal{E}^-) remain, however, essentially unaffected by μ .

The Luttinger condition that the interaction U does not alter the number of quasiparticle states inside the Fermi surface is obviously satisfied by the present construction. It follows that if the system would have exactly 2 electrons per site (the “ionic” case), the Fermi level ϵ_F would fall precisely in this gap and produce an insulating (semiconducting) ground state. [It can be seen, from (27) and (28), that the magnitude of the gap depends only weakly on the number of electrons per site.] Turning now to a quite different regime, $D_- < 0$, the connection with the $U=0$ case leads us to expect a gap somewhat larger than $|D_-|$. This is indeed found, as shown in Fig. 3. This result is relevant for the insulating gap of the “black” (low-pressure) phase of SmS.

The spectral gap was obtained under the condition that $V_k \neq 0$ for *all* k 's. It is now clear that this gap must vanish if V_k vanishes *both* for some $\epsilon_k > \epsilon_f + \mu$ and for some $\epsilon_k < \epsilon_f + \mu$. (In an actual band structure, there can be more than one type of symmetry point at which V_k vanishes.) It is also plausible (although not yet convincingly demonstrated) that a finite dispersion for the f band ($\epsilon_{fk} \neq \epsilon_f$) can contribute to gap closure.^{11,30(a)}

In the metallic case with more than 2 electrons per site, the geometric construction in Fig. 1 still applies and shows that ϵ_F still falls just above the upper gap edge, in a region of high state density. (The analog of Fig. 1 for the present case is so similar that this is not shown separately.) The renormalization of V_k by $(1-\xi)^{1/2}$ leads to a more flat lower part of \mathcal{E}^+ , and thus to an increased effective mass at ϵ_F (m^* raised from 19.1 to 37.9, for the parameters of Fig. 1). This mass enhancement effect is obviously strongest in the Kondo regime, where extreme enhancements ($\geq 10^2$) may be attained. This can be seen in Fig. 3.

The “ f weight” of each quasiparticle, as appropriate for valence-photoemission spectroscopy and bremsstrahlung isochromat spectroscopy (BIS), is given by the square of the appropriate f -transition amplitude, $\langle \Psi_{k\sigma}^{N_e+1} | \eta_{fk\sigma}^\dagger | \Psi_g^{N_e} \rangle$ or $\langle \Psi_{(k\sigma)-1}^{N_e-1} | \eta_{fk\sigma} | \Psi_g^{N_e} \rangle$ (N_e denotes electron number). Conduction-electron weights are defined similarly. By diagrammatic analysis we find these weights to be

$$\mathcal{W}_{ck}^+ = \frac{\mathcal{D}}{\mathcal{D} + A_k^2} = 1 - n_{k\sigma}, \quad (41)$$

$$\mathcal{W}_{ck}^- = \frac{A_k^2}{\mathcal{D} + A_k^2} = n_{k\sigma}, \quad (42)$$

$$\mathcal{W}_{fk}^\pm = (1-\xi) \mathcal{W}_{ck}^\mp, \quad (43)$$

where the superscripts (\pm) refer to the quasiparticle states \mathcal{E}_k^\pm . These weights can be combined with the energies \mathcal{E}_k^\pm [as shown explicitly in Ref. 30(b)] to obtain the spectroscopic conduction-electron and f -electron state densities (per spin, per site),

$$\rho_c^\sigma(E) = \frac{1}{W}, \quad (44)$$

$$\rho_f^\sigma(E) = \frac{V^2(1-\xi)^2}{W(E-\mu)^2}, \quad (45)$$

within the \mathcal{E}^\pm band limits, and zero elsewhere. The f spectral density is therefore concentrated around $E=\mu$, and consists of two sharp peaks separated by a gap. These results are quite similar to those of the “Hubbard I” Green’s-function approximation.³⁰ The corresponding Green’s-function expressions can be obtained from those of Ref. 30(b) by making the replacements $\epsilon_f \rightarrow \tilde{\epsilon}_f$ and $n_{j\sigma} = 1 - \frac{1}{2}\xi \rightarrow 1 - \xi$.

From (41)–(43) we see that $\mathcal{W}_{fk}^+ + \mathcal{W}_{fk}^- = 1 - \xi$, so the “total” f spectral intensity contributed by the quasiparticles is strongly diminished in the Kondo regime.⁵⁸ Also in the Kondo regime the f peak is narrowed, by $1 - \xi$, and it is centered near ϵ_F rather than ϵ_f . Apart from the gap near its center, this peak therefore has all of the qualitative features of the so-called Kondo peak (or Abrikosov-Suhl resonance) found near the Fermi level in Green’s-function treatments of single-impurity models⁵⁹ and also in experiments on Ce and its compounds.⁶⁰ In addition, however, and in agreement with the Ce data and these single-impurity studies, there is also a nonquasiparticle contribution to the f spectral intensity. This arises because the sudden addition or removal of an f electron can break up the delicate correlations which produce the quasiparticles. This “continuum contribution” can be treated by the resolvent technique of Gunnarsson and Schönhammer,¹⁸ with some simple modifications indicated by diagrammatic analysis. Formal similarity to the single-impurity case indicates that in the Kondo regime this contribution should produce a broad peak centered near the bare f level ϵ_f . This will require detailed numerical study, and will be reported elsewhere.

Although we have emphasized that dramatic changes can occur when $U=0$ is replaced by $U=\infty$, particularly in the Kondo regime, the opposite viewpoint should not be overlooked. By substituting $\mu=0$, $\mathcal{D}=1$ (and thus $\xi=0$) in all of the spectral formulas, (36)–(45), we obtain the corresponding results for the simple $U=0$ case. In this sense the effect of U on spectral properties is relatively gentle. (This is another aspect of the analytic continuity which underlies the Luttinger picture.) We consider this to be the reason for the rather good agreement between most of the observed de Haas–van Alphen frequencies of CeSn₃ and the results of a conventional band calculation.⁶¹

V. TWO-PARAMETER THEORY

Our “two-parameter” trial wave function is

$$\Psi = \prod_j \left\{ 1 + \sum_{\sigma} \left[\left(1 + \sum_{k'} b_{jk} \eta_{j\sigma}^{\dagger} \eta_{k'\sigma} \right) \times \sum_k a_{kj} \eta_{k\sigma}^{\dagger} \eta_{j\sigma} \right] \right\} |\Phi_c \Phi_f\rangle. \quad (46)$$

This form is motivated by the following line of reasoning: Suppose for conceptual simplicity that ϵ_f lies in the perturbative regime. Then V_k will induce some weak virtual transitions $j\sigma \rightarrow k\sigma$ with $k > k_F$. Due to the resulting partial emptiness of $j\sigma$, other transitions $k'\sigma \rightarrow j\sigma$ will now be possible for $k' < k_F$. These steps lead to an $n_{k\sigma}$ distribution with $0 < n_{k\sigma} < 1$ everywhere. At this stage it becomes appropriate to drop the $k > k_F$, $k' < k_F$ restrictions for all subsequent transitions involving $j' \neq j$. For each k there is now a new variational parameter B_k , in addition to A_k , whereby the outcome of all the competing "filling" and "emptying" processes can be optimized.

Formulas for all of the required expectation values are determined by a straightforward extension of the previous approximate diagrammatic analysis. For each k there are now two coupled equations for the optimum A_k and B_k . These equations involve *four* "basic parameters" (analogues of ξ and μ), which are themselves integrals over functions of the other A 's and B 's. The formulas are rather complicated, and numerical methods are required throughout. The details will be presented elsewhere.

Ground-state properties of this version are compared with the one-parameter version in Figs. 2 and 3. Barely visible in Fig. 2 is a slight (1–2%) emptying of the conduction states $k < k_F$. The energy is everywhere lower, as expected for a more flexible Ψ . Also, the falloff rate in the Kondo regime is noticeably slower for both $\langle H \rangle_{\text{int}}$ and $1 - \xi$. The latter features are consistent with exact Beth-ansatz results for the single-impurity Anderson model, as discussed further in Sec. VIF.

The quasiparticle spectrum for $D_- = 1.55$ eV (in the Kondo regime) is shown in Fig. 4. The effective mass is now considerably larger than for the one-parameter case ($m^* = 79.5$, as compared to the previous 37.9, for the same parameters as Fig. 1). A prominent new feature is the strong downward shift of the high- k part of \mathcal{E}_k^+ . This is understandable on physical grounds, since an "extra" electron placed in a high-energy ϵ_k orbital now has the opportunity to lower its energy by transfer into f orbitals via B_k . But since the resulting \mathcal{E}_k^+ 's are still far above ϵ_F , there is probably very little effect on thermodynamic properties. Another interesting result of this new " B_k channel" is that the f transition probability \mathcal{W}_{fk}^+ is strikingly enhanced for the upper part of the \mathcal{E}_k^+ spectrum. The function \mathcal{W}_{fk}^+ is plotted at the bottom of Fig. 4; it is obviously quite different from the corresponding one-parameter result (43). This enhancement is significant only in the Kondo regime. This combination of \mathcal{E}_k^+ flattening and \mathcal{W}_{fk}^+ enhancement, in the Kondo regime, now leads to a significant quasiparticle contribution to the f spectral weight near ϵ_f . The present quasiparticle f spectral intensity is too singular to plot directly, so instead we present in Fig. 4 the subband cumulative weights

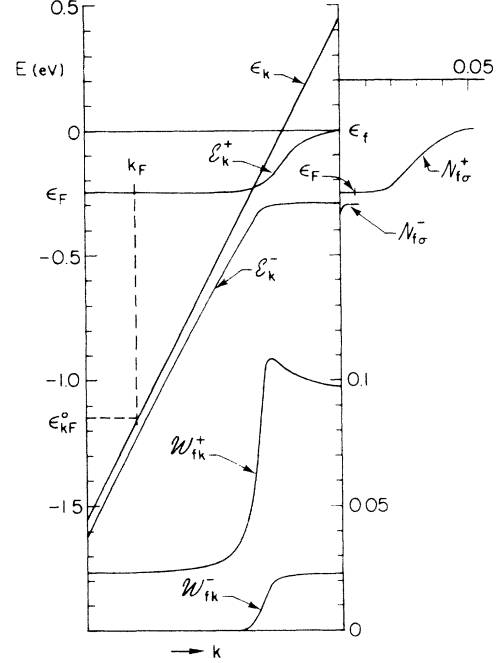


FIG. 4. Quasiparticle spectrum for two-parameter model, in Kondo regime ($D_- = 1.55$ eV). Left-hand scale is for ϵ_k and the \mathcal{E} 's; right-hand scale is for the \mathcal{W} 's.

$$\mathcal{N}_{f\sigma}^{\pm}(E) = \int_{-\infty}^E \rho_f^{\sigma\pm}(E') dE'. \quad (47)$$

There is also a "continuum contribution" to the f spectral intensity, giving a broad ϵ_f peak (not shown), as in the preceding one-parameter case. This has not yet been adequately studied.

This finding of two f -intensity regions, near ϵ_F and ϵ_f , raises the question of whether the "two-peak" valence x-ray photoemission spectroscopy (XPS) structures of Ce and its compounds⁶⁰ might be satisfactorily explained in this manner. This is presently unclear. There is now a strong indication that the finiteness of U (i.e., $U < \infty$) will be significant here,⁶² and it is also possible that a one-site $4f$ - $5d$ Coulomb term U_{fd} may strongly affect the spectrum.⁶³

VI. DISCUSSION

A. Periodic-Fermi-liquid features

An explicit realization of the Luttinger picture of a periodic Fermi liquid has been presented. There is a sharp Fermi surface, characterized by a discontinuity in the distribution of conduction-state occupation numbers $n_{k\sigma}$. The condition of infinite quasiparticle lifetime at the Fermi surface is satisfied trivially, because quasiparticle lifetime effects have not been considered (see Sec. VIG). The one-to-one correspondence between the interacting ($U = \infty$) and noninteracting ($U = 0$) quasiparticle states is enforced by construction. This automatically preserves the Luttinger sum rule: The number of states inside the Fermi surface is identical to the total number of electrons. All of these features follow from the assumption of ana-

lytic continuity when the interaction U is gradually (adiabatically) “switched on,” as shown in detail by Luttinger.⁸ Moreover, in the ground states of both of our variational models the true conduction-state occupation-number distribution $n_{k\sigma}$ is built up out of *separate* contributions from each of the occupied quasiparticle states. Here, too, there is an obvious correspondence with the elementary $U=0$ case. A significant difference from the $U=0$ case, however, is that the details of each quasiparticle now depend on the quasiparticle occupation numbers of *all* of the quasiparticle states. This dependence is carried by the “basic parameters;” in the one-parameter version the latter are ξ and μ . This aspect is discussed further in several of the following subsections.

B. Band-theoretic aspects, hybridization gap

This “adiabatic correspondence” carries over into the form of the quasiparticle excitation spectrum, which can therefore be characterized as a renormalized band theory. In the one-parameter version this renormalization aspect is quite simple and straightforward; after the replacements (39) and (40), one is left again with the elementary band-theoretic result (3). [The quasiparticle contribution to the f spectral density is, however, reduced by a factor of $1-\xi$, as compared to ordinary band theory. The renormalization (40) and a shift similar to (39) have also been obtained by the functional-integral method.⁴⁹] This is apparently the reason for the considerable success of band theory in accounting for the de Hass—van Alphen frequencies seen in CeSn_3 .⁶¹ In the two-parameter version the band renormalization cannot be characterized as simply as in (39) and (40); note the prominent distortion of the upper part of the \mathcal{E}^+ band in Fig. 4.

The spectrum typically contains a hybridization gap, just as in the $U=0$ case. In the ionic case, with just 2 electrons per site (as appropriate for SmB_6 , SmS , and YbB_{12}), the above sum-rule feature forces the Fermi level to fall precisely in this gap. In real materials, however, there may not always be a true gap. (This appears to be the case for “gold” SmS .) The gap will close if $V_k=0$ at suitable points within the Brillouin zone, and it is often speculated that a finite dispersion within the f -band manifold can also contribute to gap closure. Orbital degeneracies (both d and f) also complicate the situation, and can eliminate the gap, but crystal-field splitting and band structure can sometimes have the effect of removing these degeneracies, and thus restore the simplicity of the present orbitally nondegenerate model.¹¹ The “renormalized band” or “renormalized hybridization” interpretation also becomes more subtle when Hund’s-rule coupling and crystal-field splittings are taken into account.⁶⁴ This is because these ionic features eliminate or strongly modify many of the band-theoretic channels for f -conduction hybridization. For the present purposes, therefore, it is convenient to think of these ionic features as already incorporated within the “ $U=0$ ” reference Hamiltonian.⁶⁴

C. Lowest-temperature properties: γ and χ_0

Up to this point, only zero-temperature properties have been considered. However, the procedure for deriving the

quasiparticle spectrum amounts to altering the *quasiparticle occupation number*, $n_{\text{qp}}^{\pm}(k,\sigma)$, of one state at a time [see Eq. (37)]. In the ground state these $n_{\text{qp}}^{\pm}(k,\sigma)$ ’s are all either zero or unity. (This contrasts with the true conduction-state occupation numbers, where in general $0 < n_{k\sigma} < 1$, as is fully manifested in the two-parameter theory.) The path to nonzero temperature for this theory (either version) therefore seems clear. It appears that one must simply populate the various quasiparticle states with $n_{\text{qp}}^{\pm}(k,\sigma)$ ’s given by Fermi functions of the corresponding $\mathcal{E}_{k\sigma}^{\pm}$ ’s, and then recalculate everything self-consistently. A problem arises at higher temperatures (see Sec. VI H), but for very low temperatures, where only \mathcal{E}_k^+ excitations are significant, this procedure is correct. At the lowest temperatures, $T \rightarrow 0$, two properties are of particular interest: γ , the linear specific-heat coefficient, and χ_0 , the $T=0$ limit of the magnetic susceptibility. These will now be discussed.

Consider the formulas for ξ and μ , (27) and (28). At finite T , each $k\sigma$ term should be weighted by $[1-f(\mathcal{E}_{k\sigma}^{\pm})]$, where f is the Fermi function. The functions being weighted are smooth, so there is no change in ξ or μ to first order in T . It follows that $\delta\xi$, $\delta\mu$, and therefore the δA_k ’s, are *all* of order T^2 . Thanks to the stationarity of $\langle H \rangle$ with respect to each A_k , the changes $\delta A_k \sim T^2$ alter $\langle H \rangle$ only in order T^4 . One can therefore use the zero-temperature A_k ’s, ignoring these δA_k ’s, because γ is determined by the change of $\langle H \rangle$ in order T^2 . We now note that each addition of a quasiparticle $k\sigma$ above ε_F increases $\langle H \rangle$ by $\mathcal{E}_{k\sigma}^+$, and likewise each removal of a $k'\sigma'$ quasiparticle decreases $\langle H \rangle$ by $\mathcal{E}_{k'\sigma'}^+$. The net change in $\langle H \rangle$ (from its $T=0$ value) is therefore related to the \mathcal{E}^+ spectrum in the same manner as in elementary band theory. We thus recover the standard band-theoretic formula

$$\gamma = \frac{\pi^2 k_B^2}{3} \rho(\varepsilon_F), \quad (48)$$

where $\rho(\varepsilon_F)$ is now the total (spin-summed) *quasiparticle* density of states at ε_F .

The logic for the zero-temperature magnetic susceptibility is very similar, except that $k_B T$ is replaced by the magnetic energy $\mu_B \mathcal{H}$. Assuming $g=2$ for both the conduction and localized orbitals, there is no change in $\varepsilon_{k\sigma} - \varepsilon_{f\sigma}$. The changes δA_k are therefore due only to the changes $\delta\xi$ and $\delta\mu$, which are driven by the altered integration limits arising from $\sum_{k,\sigma} \Theta(\mathcal{E}_{k\sigma}^+ - \zeta)$, the energies $\mathcal{E}_{k\sigma}^+$ being shifted by $-(+)\mu_B \mathcal{H}$ for $\sigma = \uparrow(\downarrow)$. (Θ is the step function, and ζ is the chemical potential.) It follows that $\delta\xi$, $\delta\mu$, and therefore the δA_k ’s, are all of order $(\mu_B \mathcal{H})^2$. These δA_k ’s alter $\langle H \rangle$ only in order $(\mu_B \mathcal{H})^4$, and can thus be neglected. We therefore again obtain the standard band-theoretic result,

$$\chi_0 = \mu_B^2 \rho(\varepsilon_F). \quad (49)$$

It follows that the Wilson ratio,

$$R_W = \frac{\pi^2 k_B^2}{3\mu_B^2} \frac{\chi_0}{\gamma}, \quad (50)$$

is just unity.

The corresponding results for the two-parameter version are somewhat different. The logic for γ is essentially the same, except that ξ and μ are replaced by a set of *four* "basic parameters" which determine all of the A_k 's and B_k 's. We again obtain the simple formula (48). [It must be noted, however, that $\rho(\epsilon_F)$ is now quantitatively different; this can be seen from the m^* results in Fig. 3.] In contrast, the calculation of χ_0 is now far more complicated, and the result is not expected to agree with (49). The Wilson ratio is therefore not unity, and is instead expected to be a function of D_- or ξ .

D. The effective mass

In Secs. II and IV the effective mass m^* was defined as the relative enhancement with respect to the ϵ_k spectrum, thus

$$\frac{1}{m^*} = \left. \frac{d\mathcal{E}_k^+}{d\epsilon_k} \right|_{\mathcal{E}_k^+ = \epsilon_F} \quad (51)$$

The quasiparticle density of states is therefore

$$\rho(\epsilon_F) = \frac{2}{W} m^* \quad (52)$$

The asymptotic forms (33) can be used to obtain a significant analytical relation connecting ξ to m^* , and thus to γ and χ_0 . By expressing $\mathcal{E}_{k\sigma}^+$ in terms of y , from (25), (26), and (36), and performing the differentiation (51), one finds

$$m^* = 2(y_-^2 + 1)^{1/2} \hat{A}_- \quad (53)$$

in the notation of (27) and (28). Throughout the VF and Kondo regimes (i.e., for ϵ_f above the perturbative-VF crossover region) one has $y_- \gg 1$, and thus from (33)

$$m^* \approx (2y_-)^2 \quad (54)$$

Turning now to (27), we express this as

$$(W/2 |V|) \xi(1-\xi)^{-1/2} = \hat{A}_- - \hat{A}_+ \approx 2y_- \quad (55)$$

again using (33). We thereby obtain

$$m^* \approx \frac{W^2}{2V} \frac{\xi^2}{1-\xi} \quad (56)$$

which relates γ and χ_0 to the average valence. This relation was derived previously, for a single impurity.⁶⁵

In spite of the approximations involved in phenomenological applications (mainly, constant V_k and constant $\rho_0^{\sigma} = W^{-1}$, independent of the material), this relation is qualitatively well satisfied by a series of intermetallic Yb compounds.⁶⁶ It is noteworthy that within this series χ_0 varies by 2 orders of magnitude. The lesson is that ξ , or equivalently ϵ_f or D_- , is just as important here as the more obvious "resonance-width" parameter $\Gamma = \pi V^2 \rho_0^{\sigma}(\epsilon_F) = \pi V^2 / W$ (also denoted by Δ), or the ratio W/Γ . In more refined single-impurity studies, and apparently also in the two-parameter version, m^* is found to be even more singular than (56) as $\xi \rightarrow 1$. This is discussed in Sec. VI F.

Many previous phenomenological discussions of VF

materials have focused on an effective fluctuation temperature T_f (generally loosely defined), as a scaling temperature relevant for comparing VF compounds.⁶⁷ In view of (48)–(56), the definition

$$k_B T_f = 1/\rho(\epsilon_F) \quad (57)$$

seems appropriate. We note that in the Kondo regime this definition leads to

$$k_B T_f = |N^{-1} \langle H \rangle_{\text{int}}| \quad ,$$

for the one-parameter model, and thus T_f agrees with a reasonable definition for T_K , the Kondo temperature, as discussed further in Sec. VII. Several other definitions of a characteristic temperature are reviewed in Refs. 13, 14, and 67. To summarize briefly: Wilson has defined a low-temperature scale parameter T_0 via

$$\chi_0 = \mu_B^2 / \pi k_B T_0 \quad ,$$

related to his high-temperature scale T_K (his "Kondo temperature") via $T_K = 4\pi \times 0.1027 T_0$. We are effectively using

$$\chi_0 = R_W \mu_B^2 / k_B T_f \quad ,$$

where we presume $R_W = 2.0$ in the Kondo regime, thus $T_f = 2\pi T_0 = 4.87 T_K$. However, it is important to recognize that these statements all presume a very simple model with constant V_k and constant ρ_0 . In Secs. VI E and VI H we argue that the use of a *single* characteristic temperature should typically be inadequate when comparing the low-temperature properties of different materials.

We now summarize the present reasons for large values of m^* , as are typically encountered in VF materials, and the extremely large values ($\geq 10^2$) which are occasionally found—the latter leading to the designation "heavy-fermion" materials.^{68,69} Consider first the $U=0$ case shown in Fig. 1. Hybridization alone produces bands with extensive flattened regions, and can easily account for a mass enhancement of, say, 1 order of magnitude. Using (54) with $\mathcal{D}=1$, $\mu=0$ gives $m^* \approx (D_-^*/V)^2$, where $D_-^* = -\epsilon_{kf}^0$ is the separation between ϵ_f and the bottom of the "active" (k_+) part of the conduction band. However, electron conservation implies that $D_-^* \approx W\xi/2$ in the VF regime (this is exact for $V=0$), whereby $m^* \approx (W\xi/2V)^2$. Then, in the one-parameter model, V^2 is effectively reduced by the factor $1-\xi$, from (40), thus giving (56). A value $\xi \sim 0.9$, say, therefore provides another order-of-magnitude enhancement. Finally, we turn to the two-parameter model, and observe from Fig. 3 a *further* enhancement, by a factor which is rapidly increasing in the Kondo regime, and which can amount, there, to *another* order of magnitude. We conclude that very large m^* values are, formally, quite easy to explain. It might thus appear that arbitrarily large values are possible. In reality, however, there is some physical upper limit because, as ξ approaches unity in the Kondo regime, $\langle H \rangle_{\text{int}}$ becomes smaller than the interaction energy that the system can achieve by transforming to a phase with RKKY coupling between magnetic moments which are at least partially unquenched.^{38,40,41,50}

The physical origin of the "heaviness" can be under-

stood as follows: In the ground state, the $k < k_F$ occupied orbitals of Φ_c constitute a simple metallic state of “non-binding” electrons. The remaining $k > k_F$ conduction orbitals are partially occupied by electrons originating from Φ_f ; these are “binding and screening” electrons. [There is exactly one screening and binding electron for each f^1 configuration, thus the number of such electrons per site is ξ ; see (14) and Fig. 2.] Now consider the $k (< k_F) \rightarrow k' (> k_F)$ promotion of an “unbound” electron. The binding and screening component now finds k' replaced by a *lower-lying* state k , which thus increases the total binding energy. The heaviness arises because of a near cancellation between the bare excitation energy, $\varepsilon_{k'} - \varepsilon_k$, and this binding-energy increase. This interpretation follows directly from (35).

E. Low-temperature properties and coherence

In contrast to the strict $T \rightarrow 0$ limit treated above, we now consider the qualitative T dependence of various properties at small but finite temperature, $T \lesssim T_f$. The behaviors of some of these properties (“ γ ” equal to specific heat divided by temperature, electrical resistivity, and thermopower) have been cited as evidence for periodic coherence,^{70,71} i.e., breakdown of the independent-site picture which has been so successful at higher temperatures. (The Luttinger properties—insulating gap or sharp Fermi surface—are, of course, also strong evidence for coherence.) Viewed from the low-temperature standpoint, there is evidently a breakup of coherence with increasing temperature. One of the goals of this discussion is to identify the mechanism responsible for this breakup of the Fermi-liquid coherence.

It is well known that for the “ionic” compounds (SmB₆, SmS, YbB₁₂, TmSe), there is considerable phenomenological evidence for simple hybridization models of the present type.^{11,72,73} There is also some evidence⁷⁴ suggesting a similar model for intermetallic compounds, where the electron number necessarily keeps the Fermi level ε_F away from the hybridization gap (or pseudogap). The following discussion is directed towards intermetallic compounds. We focus on the “heavy-fermion” (very low T_f) materials, because their gap-related behaviors are least likely to be overlapped by anomalies due to crystal-field excitations, or by phonon effects. Our procedure is to begin with simple assumptions, compare their consequences with available data, and then attempt to draw some useful conclusions about the roles of complicating aspects in real materials.

1. Specific heat

We start with the simple constant- ρ_0 , constant- V_k model used above. This gives a *total* state density,

$$\rho(E) = d(\text{number of quasiparticle states})/dE,$$

of the form

$$\rho(E) = \frac{2}{W} \left[1 + \frac{\tilde{V}^2}{(E - \tilde{\varepsilon}_f)^2} \right], \quad (58)$$

in the notation of (39) and (40). It follows that

$$\rho''(\varepsilon_F) = \frac{d^2\rho}{dE^2} \Big|_{E=\varepsilon_F} > 0. \quad (59)$$

It therefore seems obvious that “ γ ” = C/T should initially rise quadratically, before leveling off and decreasing with increasing T . This behavior has been observed,^{71,75} but so far only in heavy-fermion systems (CeAl₃, CeCu₆, and some CeCu₂Si₂, samples) corresponding to very low T_f . (The peak temperatures are extremely low, only 0.27–0.5 K.) In such cases $\rho(E)$ has extremely sharp spikes, and it should therefore be very sensitive to smearing by alloying. The nonmonotonic behavior of C/T was indeed found to be easily destroyed by alloying.⁷¹

At “high” temperatures, $T \gg T_f$, the present $\rho(E)$ predicts a rapid decrease of C/T towards an asymptotically constant background, from the ρ_c of (44), together with the rising phonon contribution. For heavy-fermion materials, much of the available C/T data⁶⁹ corresponds to this $T \gg T_f$ regime, and is consistent with the present expectation.

In the crossover temperature range, $T \sim T_f$, one might expect that a gap should lead to an initial decrease of C/T followed by a second peak, or at least a shoulder, arising from the peak in the \mathcal{E}^- contribution at the far side of the gap. A simple estimate (see below) suggests that the second peak should be found at up to an order-of-magnitude higher temperature than the first peak. The available data^{69,75} do show at least hints of “second” features, gentle peaks in C whose center positions range from 2 to 4 K, for the heavy-fermion materials CeAl₃, CeCu₂Si₂, CeCu₆, and UBe₁₃. (There is no “first” peak in UBe₁₃, presumably because this is cut off by the superconducting transition.) These second features show up much more clearly in C than in C/T ; in the latter they are no more than faint shoulders. (It is not clear to us whether a faint shoulder in C of CeAl₃, at 4 K, is due entirely to a magnetic impurity.⁷⁵)

Additional information may perhaps be obtainable from measurements of the effect of a magnetic field on C/T .^{69,71} For $T \ll T_f$ the effect of a magnetic field is very simple; this just produces a rigid splitting of $2\mu\mathcal{H}$ between the \uparrow and \downarrow state densities, where this μ is the effective moment of the (presumed) crystal-field ground-state doublet. The split-band picture indicates that \mathcal{H} should *reduce* the height of the first peak. This is the case for all three materials (CeAl₃, CeCu₂Si₂, and CeCu₆) in which this first peak has been seen. In the “high- T ” ($T \gg T_f$) regime, it would seem reasonable to replace $\rho(E)$ by a *single* peak of Lorentzian form. The effect of \mathcal{H} should then be to broaden this peak, and thus to now *increase* C/T . This, too, is consistent with all of the available data,⁶⁹ except for the “paramagnon” ($T^3 \ln T$ specific heat) material UPt₃. A split-band model has already been used⁶⁹ to analyze some of this data, but the assumed $\rho(E)$ form did not include a gap.

Some simple estimates can be made, based on the $\rho(E)$ of (58). In the Kondo regime one finds

$$\varepsilon_F - \mu \approx 2V^2(1 - \xi)/W = k_B T_f, \quad (60)$$

$$\mathcal{E}_{\text{min}}^+ - \mu \approx V^2(1 - \xi)/(D_- + \mu) \approx k_B T_f / (1 + n_-), \quad (61)$$

$$\mu - \mathcal{E}_{\max}^- \approx V^2(1 - \xi)/(D_+ - \mu) \approx k_B T_f / (1 - n_<), \quad (62)$$

where \mathcal{E}_{\min}^+ and \mathcal{E}_{\max}^- are the gap edges, and $n_< = 2N_</N$ is the number of “metallic” electrons per site contained in the Φ_c of (14). ($N_<$ is the number of $k < k_F$ states.) It follows that the gap width, $\mathcal{E}_{\min}^+ - \mathcal{E}_{\max}^-$, is roughly $2k_B T_f$, and that the position of the “first peak” in C/T is determined by

$$\epsilon_F - \mathcal{E}_{\min}^+ \approx k_B T_f n_< / (1 + n_<). \quad (63)$$

One might naively expect that the second-peak/first-peak temperature ratio should be roughly

$$\frac{\epsilon_F - \mathcal{E}_{\min}^-}{\epsilon_F - \mathcal{E}_{\min}^+} \approx \frac{1 + (1 - n_<)^{-1}}{n_< / (1 + n_<)} \sim \frac{2}{n_<}. \quad (64)$$

From this standpoint the observed peak ratios (ranging from 4 to 8) seem reasonable. On the other hand, the comparison with γ , via (48) and (57), presents a problem. The T_f corresponding to $\gamma = 1.0$ J/mole K² is 27.4 K, thus the empirical T_f 's are very much larger than the observed first-peak positions.

We have carried out a series of simple model calculations in order to test these ideas more quantitatively.⁶⁴ For the above constant- ρ_0 , constant- V_k model (58), there were two significant results. The temperature of the first peak (in C/T) is very low, only around 10% of $(\epsilon_F - \mathcal{E}_{\min}^+)/k_B$. (Compare with the Schottky anomaly ratio of 0.42.) Together with (63), this may be adequate to resolve the “large- T_f , small first-peak temperature” problem just noted. On the other hand, the height of the C/T peak was very small, exceeding the $T=0$ value by only a few percent of the latter, in contrast to the several tens of percent seen experimentally.

We have tried to remove this discrepancy by adding more realistic features to the model. We substituted a semielliptic conduction-state density,

$$\rho_0(\epsilon) = (8/\pi W)[1 - (2\epsilon/W)^2]^{1/2}.$$

This rounded off the tips of the sharp spikes in $\rho(E)$, but it also pushed ϵ_F a bit farther from the gap edge, leaving the specific heat almost unchanged. [The sign change for ρ'' was extremely close to the gap edge, from which we infer that (59) should usually remain valid.] We also considered the temperature dependence of the parameters ξ and μ , which make the quasiparticle energies temperature dependent. At low temperatures, the temperature dependence of the chemical potential ξ (which plays a major role in the specific-heat calculation) was altered by just the same amount as that of the \mathcal{E}_k^+ 's near ϵ_F . This left the important differences, $\mathcal{E}_k^+ - \xi$, which enter in the Fermi function, essentially unchanged. (This must obviously be so, at least for $T \rightarrow 0$, to conserve the number of electrons.) The resulting change in specific heat was insignificant. We then turned to the k dependence of V_k , considering various plausible assumptions. Since d and f orbitals have opposite parity, we first tried $V_k \sim \sin(\pi k/k_{\max})$, as compared to $\epsilon_k \sim \cos(\pi k/k_{\max})$, whereby $V_k \sim [1 - (2\epsilon_k/W)^2]^{1/2}$. This allowed the gap to collapse. There were still two rounded peaks in $\rho(E)$, but

this ρ now vanished only at the point $E = \bar{\epsilon}_f$, leaving only a pseudogap. The first peak in C/T disappeared completely.

We did manage to find a model which is useful in explaining the large magnitudes of the observed first peaks, and yet remains plausibly consistent with the requirements of band theory. This is based on the explanation for the insulating gap of SmB_6 .¹¹ The present model has a simple (negative) band dispersion, $\epsilon_k \sim +\cos(\pi k/k_{\max})$, but $V_k \sim \sin(\pi k/2k_{\max})$ is more subtle. Of course the latter vanishes at $k=0$ (the Γ point), due to the opposite parity of d and f orbitals, but this V_k now has its maximum magnitude at the zone boundary. The monotonic increase of $|V_k|$ causes the \mathcal{E}^+ quasiparticle band to become *extremely flat* near the zone boundary, and thus to produce an extremely sharp spike in $\rho(E)$. For a given k_F , the contrast between the maximum $\rho(E)$, and $\rho(\epsilon_F)$, can thus be larger than for the case of constant V_k . This leads to a more prominent first peak. The temperature of this peak is also further reduced, as compared to (57).

Even with this mechanism, however, in order to obtain a peak magnitude comparable to observation (20% rise beyond the γ at $T=0$ for CeCu_6 , 60% for CeAl_3 , 90% for CeCu_2Si_2) we found it necessary to have k_F rather small, not more than $\frac{1}{4}$ of the zone-boundary value k_{\max} . A plausibility argument that such a feature should be found in the materials with the “heaviest” fermions is given in Ref. 64. The band-theoretic reason for the slower k dependence of V_k (in SmB_6) is also outlined there, together with the suggestion that this might be a rather common phenomenon among rare-earth and actinide intermetallics.⁶⁶ These speculations can and should be tested by means of suitably modified band calculations, as explained in Ref. 64.

Although this model appears to be adequate for the first peaks (in C/T), we find that it fails to explain the second peaks (in C). (The sharpening of the \mathcal{E}^+ state density is accompanied by a “dulling” of the \mathcal{E}^- state density.) To explain both specific-heat features simultaneously, it appears necessary to assume a conduction-band structure with *more than one* branch intersecting $\bar{\epsilon}_f$ and the nearby Fermi level ϵ_F . This is of course very likely to be true for the complicated materials we are dealing with. We find that the simple renormalized hybridization picture becomes generalized in the obvious manner. [Regardless of the number of conduction branches, *all* of the V_k 's become renormalized by the same factor $(1 - \xi)^{1/2}$.] It is therefore easily seen that any additional “bare” conduction branches will lead to new quasiparticle bands. The latter will overlap the \mathcal{E}^+ , \mathcal{E}^- gap, and thus reduce it to a pseudogap, but the assumed sharp spike in the \mathcal{E}^+ density need not be disturbed significantly. The new quasiparticle bands should generally have Lorentzian-like peaks in their state densities, centered near μ (i.e., near $\bar{\epsilon}_f$), and these $\rho(E)$ peaks may well account for the second peak in C . Data which supports this conjecture is described below.

2. Resistivity

In the same spirit, we begin with a “simplest” assumption for the electrical resistivity. We assume perfectly

periodic quasiparticles, and no interactions between these quasiparticles. The resistance is then due entirely to impurities and crystal imperfections. In this case we can use a well-known conductivity formula,⁷⁷

$$\sigma(T) = \int \bar{\sigma}(E) \left[-\frac{\partial f}{\partial E} \right] dE, \quad (65)$$

where f is the Fermi function,

$$\bar{\sigma}(E) = \frac{1}{3} e^2 \lambda(E) v_{\text{gr}}(E) \rho(E), \quad (66)$$

and e is the electron charge.

The present application is based on the fact that transport and scattering of electrons must be attributed entirely to the band or "conduction" orbitals. Although this statement is quite obvious, its consequences must be examined carefully:^{30(b)} (a) The localized orbitals have a major effect on the group velocity v_{gr} . During the fraction of time that an electron resides in a localized orbital, it experiences no transport at all. The group velocities of quasiparticle states near the hybridization gap, where the localized-orbital character is strong, are therefore drastically reduced. The group velocity is

$$v_{\text{gr}} = \frac{1}{\hbar} \frac{\partial \mathcal{E}_k^+}{\partial k} = \frac{1}{\hbar} \frac{\partial \varepsilon_k}{\partial k} \frac{\partial \mathcal{E}_k^+}{\partial \varepsilon_k} = \frac{v_{\text{gr}}^c}{m^*}, \quad (67)$$

where the effective-mass enhancement m^* must now be viewed as a function of $\mathcal{E}_k^+ = E$. Differentiating (36), then using (36) again to obtain ε_k from \mathcal{E}_k^+ , we find

$$\frac{1}{m^*(E)} = \frac{(E - \mu)^2}{(E - \mu)^2 + V^2(1 - \xi)}, \quad (68)$$

assuming constant V_k . For initial orientation we neglect the k (and thus the $E = \mathcal{E}_k^+$) dependence of the conduction-band group velocity v_{gr}^c . (b) The density-of-states factor, $\rho(E)$, must be interpreted as the *total* state density,

$$\rho(E) = d(\text{number of quasiparticle states})/dE,$$

multiplied by the conduction-orbital probability $P_c(E)$ for the quasiparticles with $\mathcal{E}_k^+ = E$. This $P_c(E)$ is given by (68), as is obvious on physical grounds, and it is also equal to \mathcal{W}_{ck}^+ , Eq. (41). The result of this recipe is just $\rho_c(E)$, the renormalized conduction-state density (44) (now summed over spin), whose main difference from the bare state density ρ_0 is the presence of the hybridization gap or pseudogap. (c) In first Born approximation, the mean free path λ is determined entirely by the conduction orbitals. In higher approximations one must also consider the renormalization of the energy spectrum ($\varepsilon_k \rightarrow \mathcal{E}_k^+$), and the reduced conduction-orbital content of the quasiparticles, $P_c(E)$. The result of the latter considerations is again to replace $\rho(E)$ by $\rho_c(E)$, within the calculation of λ . We conclude that λ should not have a very strong energy dependence, and we therefore replace it by an "ordinary" E -independent conduction-band value, $\lambda(E) \rightarrow \lambda_c$. The result of this analysis is therefore

$$\bar{\sigma}(E) \approx \frac{e^2 \lambda_c v_{\text{gr}}^c}{3} \frac{\rho_c(E)}{m^*(E)}. \quad (69)$$

Phenomenologically, the first feature to notice about (65) and (69) is that σ tends to be very small. This is because m^* tends to be large, or alternatively because P_c tends to be small.⁷⁸ Next, we note that essentially all intermetallic VF materials show

$$\rho(T) = [\sigma(T)]^{-1} \approx \alpha + \beta T^2$$

at sufficiently low T , where β is positive and can be quite large in the Kondo regime. This requires that $d^2 \bar{\sigma}(E)/dE^2$ be negative at ε_F . Unfortunately, this is not so for the simplified model [(58) and (69)], where $\rho_c(E)$ is a step function and the derivative at ε_F is due entirely to (68). For the latter, we note that $(\varepsilon_F - \mu) \ll V(1 - \xi)^{1/2}$, according to (60), so the energy dependence is dominated by the $(E - \mu)^2$ factor in the numerator. The resulting strong effect of $m^*(E)$ could not be overcome by our subsequent refinements of $\rho_c(E)$, V_k , and $v_{\text{gr}}^c(\varepsilon_k) \rightarrow v_{\text{gr}}^c(E)$, in the models described above for the specific heat; $\bar{\sigma}''(\varepsilon_F)$ remained positive in every case.

It appears to us that the resolution of this impasse will require Baber scattering,⁷⁹ as was already suggested for CeAl₃ a decade ago.⁸⁰ This process involves scattering between thermally excited quasiparticles, due to the effective quasiparticle interaction. It also requires the existence of at least two quasiparticle (qp) bands, and these must have very different effective masses.⁷⁹ We have just argued, however, that two or more branches of the conduction-band manifold are indeed likely to intersect ε_F . Their combined hybridization with the f orbitals would almost certainly provide differing effective masses, the "extra" qp bands typically having smaller masses at ε_F .

Another possibility emerges when one adds the $\bar{\sigma}(E)$ expressions (69) for each of the extra qp bands just mentioned. With generally smaller m^* 's, these bands should dominate the very-low- T conductivity. It remains to be seen whether the corresponding $\bar{\sigma}''(\varepsilon_F)$'s can be negative, and sufficiently negative to resolve the discrepancy. We consider this unlikely.

At somewhat higher temperatures, the Kondo-lattice and heavy-fermion materials typically show a very steep rise in resistivity, climbing to a peak many times greater than the $T=0$ value, followed by a slow ($\ln T$, Kondo-like) decrease. (The occurrence of a further peak or shoulder at higher T , in CeAl₃, UBe₁₃, and CeCu₂Si₂, can plausibly or definitely be attributed to crystal-field excitations.⁸¹) It seems very unlikely that this enormous rise could be explained by means of $\bar{\sigma}(E)$ or Baber scattering, and for the heavy-fermion materials the energy scale is clearly too small to be associated with crystal-field excitations. The Kondo-like behavior ($\rho \sim \ln T$) obviously cannot be explained either, by any of these mechanisms. We therefore turn to the ultimate limitation of the renormalized-band or renormalized-hybridization model—a mechanism which we believe is responsible for the crossover from the low- T Fermi-liquid behavior to the higher- T "dense Kondo" behavior. (By the latter term, we mean $\ln T$ resistivity and Curie-type magnetic susceptibility.)

We recall that the \mathcal{E}^- qp branch is obtained, via (37), by altering the occupation numbers of the f orbitals (in Bloch representation) within the Φ_0 of (34). Thanks to

this “ f character,” the excitation of a qp state from this \mathcal{E}^- branch alters each one of the N sites by an amount $1/N$, which is equivalent to fully altering one site. In Sec. VII we argue that in the simplest (one-parameter) version, the nature of this alteration is to prevent hybridization and leave the site in a pure magnetic (f^1 -like or f^{13} -like) configuration. In other words, a local moment is generated, or rather, it is released from its singlet bound state. In the two-parameter version, spin-flip scattering becomes possible for this site, and we note that spin-flip scattering is the key ingredient for $\ln T$ resistivity. The details have not been worked out, but one can already see that each \mathcal{E}^- qp excitation effectively creates one site exhibiting incoherent spin-flip scattering. Excitation of a significant number of quasiparticles (a macroscopic fraction of N) from the “far” qp branch (on the side of the gap opposite from ε_F) can thus produce a drastic change in the transport properties. (This should even change the qp spectrum itself, according to Sec. VII.) Incoherent Kondo behavior is thereby “turned on” in a continuous manner with increasing T , at temperatures comparable to $(\varepsilon_F - E_{fp})/k_B$, where E_{fp} is the position of the far peak in the qp state density. It follows that this crossover temperature range is necessarily *much* higher than the temperature of the peak in C/T , as is indeed found experimentally.

A related crossover mechanism was discussed long ago by Doniach,⁷⁰ who called this “dehybridization.” This proceeds by means of a rapidly-growing ($\sim T^2$) imaginary part of the self-energy (within the Green’s function), and is thus a consequence of intraband and interband (Baber) qp scattering. We agree that this should also be present, but this is different and much less radical than the present mechanism. We have presented both empirical and theoretical arguments that the main mechanism for the Kondo crossover is the turning on of spin-flip scattering, by means of thermally generated local moments.

The present picture also explains why the temperature of the resistivity peak is typically higher than that of the second peak (in C). The former is due to the far peak in $\rho(E)$, arising from the \mathcal{E}^- branch, while the second peak comes from a “central” peak in $\rho(E)$, located near μ or $\tilde{\varepsilon}_f$, due to qp branches resulting from additional conduction-band branches. Alternatively, the discrepancy between the experimental peaks can be taken as evidence for additional conduction-band branches.

There is, however, a notable exception to this rule. In UBe_{13} the resistivity peak coincides with the second peak in C . We attribute this difference to a Γ_8 (quartet) crystal-field ground state, for the $U^{3+} = 5f^3$ configuration, together with a Γ_1 singlet ground state for the $U^{4+} = 5f^2$ configuration. We note that these assignments are quite plausible from the standpoint of general systematics,⁶⁴ even though direct evidence is lacking. We have also explained⁶⁴ how the Γ_8 quartet can be incorporated within the present type of hybridization model, simply by assuming that there are *two* spatially-different types of localized f orbitals (in addition to the two-fold spin degeneracy), which both have the “bare” energy ε_f . We shall demonstrate elsewhere that the renormalizations all follow the simple pattern of (39) and (40). The conse-

quence is then easily seen to be a new and large peak in $\rho(E)$, concentrated at μ or $\tilde{\varepsilon}_f$, and having the same “ f character” described above for the \mathcal{E}^- branch. This will turn on spin-flip scattering at a lower temperature, and thereby lower the temperature of the resistivity peak to a point near the second peak in C . The experimental agreement between these features is, in fact, quite close.^{69,82}

3. Other properties

The present picture is also supported by magnetic susceptibility, for CeAl_3 and CeCu_6 . The χ of CeAl_3 shows a mild peak at 0.7 K.⁸⁰ We argue that this arises from basically the same source as the first or C/T peak, but with the χ peak skewed to a somewhat higher T by the precursor tail of the spin-flip or “moment-unquenching” turn-on. (This presumes that the latter effect is, relatively speaking, quite strong.) There is also a shoulder in χ at 5.5 K, coinciding with a shoulder in resistivity, both of which are above the (presumed) weak second C peak around 4K.⁷⁵ Agreement between these χ and resistivity features is expected, since both should be generated by the \mathcal{E}^- peak. In CeCu_6 there is a similar agreement between the resistivity maximum, at 13 K, and a very prominent shoulder (or weak peak) in χ , but only along one crystallographic axis.⁸³

Magnetoresistance data also tend to support the present picture. In the elementary model (65)–(69), the effect of the magnetic splitting of the \uparrow and \downarrow bands, by $2\mu\mathcal{H}$, should be qualitatively similar to a temperature increase, $\Delta T \approx \mu\mathcal{H}/2k_B$, because $-\partial f/\partial E$ averages $\bar{\sigma}(E)$ over a total width of about $4k_B T$. [The maximum of $-\partial f/\partial E$ is $(4k_B T)^{-1}$.] The magnetoresistance should thus be $\Delta\rho \approx \rho(T + \Delta T) - \rho(T)$; this is $\sim \mathcal{H} d\rho/dT$, unless

$$k_B T_f \gg \mu\mathcal{H} \gg k_B T \quad (\Delta\rho \sim \mathcal{H}^2),$$

or $\mu\mathcal{H} \gtrsim k_B T_f$ (complex behavior). The prediction is obviously for $\Delta\rho$ positive at low T , then changing sign near the peak in $\rho(T)$. Now consider the Kondo behavior which enters at higher T , and its strong negative magnetoresistance which is essentially quadratic in \mathcal{H} .⁸⁴ The temperature of the sign change should thus be somewhat reduced, and should be even further reduced by increasing \mathcal{H} . This sign change and dependence on \mathcal{H} have been observed in CeAl_3 ,⁸⁵ and the sign change also occurs in CeCu_2Si_2 .^{69,86} CeCu_6 is highly anisotropic, but at 1.3 K and along one axis it does show the expected sign change with respect to \mathcal{H} .⁸³ UBe_{13} , however, has $\Delta\rho$ simply everywhere above its superconducting transition,⁶⁹ consistent with the above argument about more rapid turn-on of the Kondo behavior, although high-field measurements suggest a sign reversal at very low T (~ 0.1 K).⁸²

If the elementary resistivity treatment (65)–(69) were correct, the same $\bar{\sigma}(E)$ should be valid for use within the standard formulas⁸⁷ for other transport properties, such as thermopower and Hall coefficient. This approach gives definite sign predictions for these properties. (See an important comment about this in Sec. VII.) Both of these properties should be positive (negative) for Ce (Yb) materials. The experiments⁸⁸ generally follow these predictions at high temperatures, but for the “heavy” materials

these properties typically show sign reversals below some $T \geq T_f$. This is surprising, because the elementary approach should apparently be most reliable at the lowest temperatures. In the case of CeCu_2Si_2 , the “wrong sign” of the thermopower has been attributed to a relatively rapid temperature variation of the average valence,⁸⁹ i.e., of ξ . For the Hall effect, skew scattering has been suggested.⁹⁰ Another possibility for these low- T discrepancies is the recently-suggested “Kondo-hole” concept,⁹¹ where the absence of an “active” ion (a vacancy, or substitution by an inert ion) has a drastic effect by virtue of the strong alteration of that site. According to this picture, a defect on the active sublattice is far more effective than one on a ligand sublattice. However, recent data show the thermopower returning to the expected sign at extremely low temperatures,⁹² for CeAl_3 and CeCu_2Si_2 , thus we suspect that the explanation lies in a strong T dependence of the qp spectrum and/or ξ . This conclusion is supported by anomalies in the thermal expansion.^{80,93} We also expect that such a strong temperature dependence will emerge from a proper extension of the present work to finite T , as outlined in Sec. VIH.

Inelastic neutron scattering has been analyzed in much the same spirit as the present discussion, by Fedro and Sinha,³¹ and by Huber,³⁰ They consider quasiparticle-quasihole excitations, and they find some qualitative agreement with experiment, especially for the q dependence and T dependence of the inelastic peak.⁷⁴ We find that for such quasiparticle excitations the explicit $1-\xi$ factors for the \mathcal{W}_{fk} 's of (43) are missing; the coupling of the neutron to the quasiparticles involves only the f contents obtained from the elementary hybridization picture (using, however, the renormalized parameters \tilde{V}_k and $\tilde{\epsilon}_f$). But two more aspects need to be worked out before the present picture can be properly applied to neutron scattering, namely, the detailed temperature dependence of the qp spectrum, which arises from the \mathcal{E}^- thermal excitations (Sec. VIH), and the possibility of a significant “continuum” (nonquasiparticle) contribution.

Finally, we mention the relaxation rates seen in electron-spin-resonance, nuclear-magnetic-resonance, and ultrasonic attenuation experiments. These relaxations are all expected to proceed via quasiparticle-quasihole excitations, and in the simplest picture the couplings to the experimental probes involve only the conduction-orbital components of the quasiparticles. Each quasiparticle is thus weighted by $P_{ck} = \mathcal{W}_{ck}^+$, whereby the relevant state density is ρ_c . This ρ_c has a very ordinary conduction-band magnitude [see (44)], consistent with the lack of prominent enhancement found in electron-spin-resonance⁹⁴ and ultrasonic attenuation⁹⁵ experiments. The NMR data does show considerable enhancement, but in this case there are several known mechanisms which can introduce coupling via f -orbital components,⁹⁶ and thus involve the enhanced density $(1-\xi)^{-1}\rho_f$ [see (45)].

4. Conclusions

It now seems reasonably well established that the Luttinger picture is correct for VF materials, and also that this leads to a renormalized hybridization model for the qp spectra at $T=0$. We have therefore considered how

this basic picture, together with the expected complications of real materials (conduction-band structure, k dependence of V , crystal-field splitting, etc.) can be reconciled with the low-temperature phenomenology of “normal” heavy-fermion materials. At energies small compared to crystal-field excitations, general arguments indicate that their $\rho(E)$'s should typically have a “three-peak” type of structure. The qualitative agreement with available data seems reasonably good, in view of the expected variability and complexity of individual materials. The proposed correspondence involves some speculations about details of conduction-band structure and V_k ; these speculations can and should be tested by means of a suitable band-theoretic analysis.⁶⁴ Treatment of excited crystal-field states is described in Ref. 64.

The heavy-fermion superconductor UPt_3 departs conspicuously from the present phenomenology in several respects, and likewise for UAl_2 . The $T^3 \ln T$ terms in their specific heats seem to be signatures for paramagnon behavior, suggesting that interactions among the quasiparticles are now playing a major role. We suspect that the underlying reason why these materials behave so differently is due to breakdown of the present $U = \infty$ assumption.

For any material with only one branch of the conduction band intersecting the effective f level ϵ_f , there should be only a *single* scaling parameter,

$$T_f \sim V_{kF}^2 (1-\xi) \rho_0(\tilde{\epsilon}_f),$$

for all of the various electronic phenomena, at temperatures well below the first crystal-field anomaly. Thus, for example, data for any thermodynamic or transport property taken at different pressures should obey a *single-parameter* scaling.⁹⁷ If, however, more than one branch of the conduction band is significant here, it is at least conceivable that the V_k 's and ρ_0 's for the various branches could have different volume dependences, in which case one-parameter scaling would not necessarily apply. On the other hand, if the dominant effect of pressure is to vary $(1-\xi)$, this would tend to enforce one-parameter scaling. The crystal-field splitting will very likely have a different volume dependence than T_f , so any features involving the magnitude of this splitting should not be expected to follow a single-parameter scaling. All of the low-temperature properties depend on material-specific details, thus, in general, one should not expect any simple scaling law to accurately relate one material to another. Nevertheless, if the relevant temperature scale is large enough (in the VF regime), it may become reasonable to ignore the crystal-field splitting, and thereby come close to a simple one-parameter scaling behavior.

F. Correspondence with single-impurity results

Experimental phenomenology indicates that there must be a close correspondence between the lattice problem and the single-impurity problem, because single-impurity models have been highly successful for periodic VF materials,¹⁻³ except at the very low temperatures where coherence effects appear.^{70,71} Formally, however, it is not at all obvious that this should be the case. There are two

general results bearing on this issue, but these are of limited help: (a) Thermodynamic perturbation theory shows that an independent-site picture becomes asymptotically correct at high temperatures (but still with an indirect coupling via the chemical potential).⁹⁸ (b) For the $T \rightarrow 0$ regime, Ward-identity studies have shown that the Wilson ratio (50) for an Anderson lattice need not be the same as for the corresponding single Anderson impurity.⁹⁹ (This is consistent with the existence of magnetic ground states, and with the apparent observation of reduced Wilson ratios for the heavy-fermion superconductors.⁶⁹) In any event, we believe it is significant that the present results show a number of strong correspondences with previous single-impurity results, including both exact results from the Bethe-ansatz work and approximate results from the $(1/N_f)$ -expansion studies.

Our one-parameter and two-parameter versions correspond closely to the first and second stages of the $1/N_f$ expansion. To see this, one should focus on a single site j and consider the types of configurations being admixed, in the trial wave functions (14) and (46). The discussion of Gunnarsson and Schönhammer¹⁸ is very helpful here. For a single site, the one-parameter model is *identical* to the leading approximation, $(1/N_f)^0$, of the $(1/N_f)$ -expansion school. The two-parameter model fails to include all of the configurations to order $(1/N_f)^1$, but Gunnarsson and Schönhammer have found that the terms we omit tend to be unimportant.¹⁰⁰ We would therefore expect to differ from the "exact" $(1/N_f)^0 + (1/N_f)^1$ results by only some small percentage, and to correctly recover all of their qualitative features. This is very encouraging, because the most careful $(1/N_f)^0 + (1/N_f)^1$ results to date are qualitatively and even quantitatively in remarkably good agreement with the exact Bethe-ansatz results.²³ [However, a problem of a spurious singularity¹⁰¹ remains for dynamical properties calculated to order $(1/N_f)^1$.] The $(1/N_f)^1$ terms that we omit correspond to the sequence of (virtual) transitions $j\sigma \rightarrow k\sigma$, $k'\sigma \rightarrow j\sigma$, $j\sigma' \rightarrow k'\sigma'$, and would thus require a "three-parameter" model. This would probably be prohibitively complicated, so it is gratifying to find these indications that the two-parameter level of approximation may be reasonably accurate.

The first type of correspondence we found is between the sharp "two-peak plus gap" photoemission f -electron state density (45), near the Fermi level, and the "Kondo peak" (or Abrikosov-Suhl resonance) of the single-impurity studies. There are three aspects to be compared here: (a) In both cases the resonant structure is near but not precisely at ϵ_f . (b) The characteristic widths are of order $1 - \xi$. (c) The integrated total intensities are of order $1 - \xi$.

Our f spectral density contains both quasiparticle and nonquasiparticle contributions, corresponding to the pole and continuum terms of Gunnarsson and Schönhammer.¹⁸ The above Kondo-peak structure derives entirely from the quasiparticle contribution, which also has a surprising property: In the Kondo regime for the two-parameter version (but not in the one-parameter version), we also find some f spectral density near the bare f -level ϵ_f . This structure fades away as ϵ_f is lowered into the VF

regime, in common with the broad ϵ_f peak found for the single impurity.⁵⁹ We expect to find considerably more intensity near ϵ_f from the continuum contribution, but this remains to be studied.

Another significant correspondence is the effective-mass formula (56). The same formula [expressed as $\gamma(\xi)$ and/or $\chi_0(\xi)$] was obtained from single-impurity studies at the $(1/N_f)^0$ level.⁶⁵ In the limit $\xi \rightarrow 0$, the exact Bethe-ansatz result also agrees with this formula.²³ On the other hand, Bethe-ansatz and $(1/N_f)^0 + (1/N_f)^1$ calculations agree that, as $\xi \rightarrow 1$, $\chi_0(\xi)$ increases far more rapidly than as $(1 - \xi)^{-1}$, and in fact as an exponential,²³

$$\chi_0 \sim \exp[1/N_f(1 - \xi)].$$

The formal analyses^{23,24} indicate, however, that this much more rapid dependence of χ_0 on ξ is *not* due to a more rapid asymptotic dependence of χ_0 on ϵ_f (or D_-), but is due instead to a far slower asymptotic dependence of $1 - \xi$ on ϵ_f , namely, $1 - \xi \sim (\epsilon_f - \hat{\epsilon}_F)^{-1}$ (see below), in contrast to the exponentially-decreasing $(1/N_f)^0$ behavior seen in (30) and (31).

In spite of this formal analysis that χ_0 should have a similar asymptotic dependence on ϵ_f , we find that in the interesting range $0.6 \lesssim D_- \leq 1.7$ eV (the upper limit of the present two-parameter calculations), the m^* of the two-parameter model is increasing *far more rapidly* than for the one-parameter model; the ratio

$$m^*(\text{two-parameter})/m^*(\text{one-parameter})$$

is steadily increasing. Study of asymptotic formulas in Ref. 23 (although for χ_0 , rather than for $m^* \leftrightarrow \gamma$) indicates three sources for this enhancement: (a) The relevant parameter for asymptotic behavior in the Kondo regime is ϵ_f^* rather than ϵ_f , where ϵ_f^* incorporates an effective (constant) level shift. A part of this level shift is formally of order $(1/N_f)^1$ and thus displaces the χ_0 curves for the two approximations by a constant shift along the ϵ_f (or D_-) axis. [This shift corresponds to the $(N_f V^2 / W D_K)^{1/N_f}$ prefactor seen in the most-refined calculations of the Kondo temperature.] (b) There is a further small enhancement of the exponential prefactor, by a factor $\Gamma^{-1}(1 + N_f^{-1})$, which equals 1.13 for the present $N_f = 2$. (c) There is a difference between the regimes $2\pi V^2 / W \ll (\epsilon_f - \hat{\epsilon}_F) \ll D_K$ and $D_K < (\epsilon_f - \hat{\epsilon}_F)$ (i.e., ϵ_f above the entire conduction band). In the former regime (corresponding to $D_- \gtrsim 1.7$ eV) there is some further enhancement, by a factor $(e D_K / |\epsilon_f - \hat{\epsilon}_F|)^{1/2}$, which eventually dies away. The latter factor cannot be taken literally for $D_- \leq 1.7$ eV, but it does indicate an extra enhancement in this region. The quantitative behavior of

$$m^*(\text{two-parameter})/m^*(\text{one-parameter})$$

seems reasonably consistent, in view of the rather vague point (c). [Of course, the different Wilson ratios should also be considered when comparing our $m^* \leftrightarrow \gamma$ results with these single-impurity χ_0 results, but this will not affect the present conclusion if the two-parameter R_W is consistent with (70) below.]

There is some further correspondence for the Wilson ratio (50). The one-parameter model gives $R_W = 1$, as

shown above, in agreement with the $(1/N)^0$ studies. Although χ_0 has not yet been calculated for the two-parameter model, we expect the resulting R_W to differ from unity and to depend on ξ (or D_-). The $(1/N_f)^0 + (1/N_f)^1$ result for a single impurity is²²

$$R_W = \left[1 - \frac{1 - (1 - \xi)^2}{N_f} \right]^{-1}. \quad (70)$$

For $N_f=2$ (the present case with only spin degeneracy), this varies between 2, for $\xi=1$, and 1, for $\xi=0$. The Bethe-ansatz result¹⁰² for $N_f=2$ varies between the same limits, but is always larger than (70); the maximum difference is about 0.14 near $\xi=0.6$. The Bethe-ansatz result falls from 2.0 very slowly; in fact, $R_W > 1.99$ for $\xi > 0.81$.

Finally, we consider the asymptotic dependences of $1 - \xi$ and $\langle H \rangle_{\text{int}}$ on D_- (or equivalently, on $\epsilon_f - \hat{\epsilon}_F$) in the Kondo regime. The exponential falloffs in (30) and (31) agree with the $(1/N_f)^0$ single-impurity results. The two-parameter results for $1 - \xi$ and $\langle H \rangle_{\text{int}}$ are clearly falling more slowly, however. It has been shown²³ that the single-impurity $(1/N_f)^0 + (1/N_f)^1$ result for $1 - \xi$ agrees rather well with the Bethe-ansatz result, throughout all of the Kondo regime, and that this falls asymptotically only as $(\epsilon_f - \hat{\epsilon}_F)^{-1}$. We suggest that the actual behaviors of $1 - \xi$ and $\langle H \rangle_{\text{int}}$ can each be viewed as a sum of two contributions: (a) an exponential term similar to (30) or (31), but perhaps with a different (and slowly-varying) prefactor, and (b) an ordinary (nonexponential) function of $\epsilon_f - \hat{\epsilon}_F$, which arises from second-order perturbation in V for the B_k -type processes $k\sigma \rightarrow j\sigma$, with $\epsilon_k < \hat{\epsilon}_F$. This perturbative picture gives

$$1 - \xi \rightarrow 2V^2/W(\epsilon_f - \hat{\epsilon}_F) \quad (71)$$

and

$$\frac{1}{N} \langle H \rangle_{\text{int}} \rightarrow -\frac{2V^2}{W} \ln \left[\frac{\epsilon_f - \hat{\epsilon}_F}{\epsilon_f - D_-} \right]. \quad (72)$$

These many and fairly detailed correspondences strongly suggest that the present results are reliable.

G. The present approximations

The approximations in the present work are of several types: (a) the choice of trial wave functions Ψ , (b) the diagrammatic approximation for the expectation values and transition amplitudes, and (c) neglect of some of the quasiparticle interaction effects. None of these approximations affect electron-number conservation, which is handled precisely throughout. (This is true even before and during optimization of the variational parameters.) This feature is important for the correct placement of the Fermi level. The most obvious effect of $U = \infty$, the elimination of f^0 configurations, is also treated exactly.

Choosing a form of trial wave function Ψ is equivalent to selecting the classes of configuration admixtures to be considered. This aspect has been discussed in Secs. V and VI F. The remarkably good agreement between $(1/N_f)^0 + (1/N_f)^1$ and Bethe-ansatz results for the single-impurity problem, and the various good correspondences between these results and our lattice results (Sec.

VI F), offer considerable hope that the two-parameter level of approximation may be adequate for most practical purposes. We do, however, neglect certain terms of order $(1/N_f)^1$ (Sec. VI F). These deserve further study, although it appears that their omission is not very significant.¹⁰⁰

These optimistic statements are, however, based only on very-low-temperature ($T \ll T_f$) behavior. A number of important aspects remain to be studied, including higher-temperature behavior, the continuum contribution to the f spectral intensity, inelastic neutron scattering, and also magnetic phases and the effective RKKY interaction.

Within our diagrammatic analysis, we see only one kind of approximation. Grewe and Keiter³⁵ have emphasized that, in diagrammatic cluster-expansion terms with more than one VF site, the summations over site indices should be restricted so that no site labels can coincide. Our diagrammatic formalism is different from theirs, but it shares this "site-exclusion" feature. We have totally ignored this restriction. From this standpoint, it is difficult to understand why we have obtained such apparently-reasonable results.¹⁰³ On the other hand, the fact that our one-parameter formulas have a simple physical interpretation [Eqs. (20)–(23)] suggests that this is in some sense a consistent approximation. Obviously, further study is needed here.

There is a further motivation for refining this approximation. We would like to eventually extend the present work to finite U (i.e., $U < \infty$) in order to study (a) the "two-peak" photoemission structure of Ce and its compounds, (b) the various phase transitions of Ce, and (c) the connections with paramagnon phenomena, including the phenomenology of UPt₃ and UAl₂. Preliminary work suggests that the site-exclusion problem will have to be dealt with in order to obtain proper behavior as $U \rightarrow 0$.

Interactions between the quasiparticles should have a number of physical consequences which we have not considered. These interactions should lead to finite quasiparticle lifetimes (except on the Fermi surface at $T=0$), to Baber-scattering contributions to resistivity and other transport properties, perhaps to paramagnon effects or to collective oscillations of some sort, and possibly even to superconductivity. (The origin of the pairing interaction, in those VF materials which also superconduct, is presently unclear.) A further and very important effect of these interactions is described in Sec. VI H.

It is noteworthy that a study of quasiparticle interactions has already been carried out,¹⁰⁴ in much the spirit of this paper, for a single impurity to order $(1/N_f)^0$. There it was found that the diagonal interaction between \mathcal{E}^+ -type quasiparticles on the Fermi surface is repulsive and spin independent. It was also noted, however, that this interaction must be spin dependent in order $(1/N_f)^1$; this can be viewed as the origin of the nontrivial Wilson ratio (70). We have indeed found effects attributable to this spin-dependent interaction, in our preliminary effort to calculate χ_0 for the two-parameter version. The diagonal interactions between \mathcal{E}^+ -type quasiparticles arise via the dependence of the "basic parameters" (ξ and μ , for the one-parameter version) upon the quasiparticle occupation numbers $n_{\text{qp}}^+(k, \sigma)$, and are therefore rather straightfor-

ward (although tedious) to calculate. These interactions were considered in Sec. VIC.

The present basic strategy (variational ground state, leading to quasiparticles) has some resemblance to the Bardeen-Cooper-Schrieffer theory of superconductivity. The success of that theory suggests that neglect of quasiparticle lifetime effects should be satisfactory for many purposes.

H. The higher-temperature problem

The final point about approximations is probably the most significant. This is that the present treatment of the quasiparticle spectra is valid only when the number of \mathcal{E}^- excitations is very small, corresponding to $T \ll T_f$.

The problem is most easily visualized for the case of a single impurity. There, the analog of the \mathcal{E}^+ spectrum has been discussed by de Chatel,¹⁰⁴ while the \mathcal{E}^- spectrum reduces to just a single state (for each spin σ), namely, the state obtained by removing $f\sigma$ from the initial wave function $\Phi_f = |f\uparrow, f\downarrow\rangle$. In the one-parameter model, excitation (i.e., removal) of the \mathcal{E}_σ^- state leads to a “free-spin” state in which hybridization is totally suppressed. In the language of quasiparticle interactions, we see that the interaction of \mathcal{E}_σ^- with $\mathcal{E}_{k\sigma}^+$ is singular, because removal of the \mathcal{E}_σ^- state transforms the qp energies $\mathcal{E}_{k\sigma}^+$ into their “bare” equivalents, $\epsilon_{k\sigma}$. Moreover, removal of \mathcal{E}_σ^- forbids the excitation (removal) of $\mathcal{E}_{-\sigma}^-$. Similar statements apply for the two-parameter version, except that $\mathcal{E}_{k\sigma}^+ \rightarrow (\mathcal{E}_k^0, \epsilon_{k\sigma})$, i.e., the “same spin” $\mathcal{E}_{k\sigma}^+$ is shifted to an energy \mathcal{E}_k^0 different from the bare $\epsilon_{k\sigma}$. Also, spin-flip scattering now becomes possible, and $\xi \neq 1$.

For the lattice case, we believe that the correct physical picture at finite temperatures is that of a *diluted* (although nonstationary) system of bound singlets, the remaining sites being local moments which are effectively nonhybridizing. The assumption of complete site equivalence, valid at $T=0$, must thus be abandoned. In the language of Sec. VID, each unbound site will release one electron from the “binding and screening” reservoir (which derives from Φ_f), and transfer this into the unbound-electron (ordinary metallic) subsystem Φ_c . The resulting renormalized-hybridization picture may therefore be strongly temperature dependent. We intend to quantify this picture in future work.

Some such refinement would also be needed for materials corresponding to the present model with *less than 2* electrons per site, if, indeed, any such materials exist. The existence of such systems seems unlikely, because of the serious loss of VF correlation energy which this situation would necessarily produce. If we accept the assumption that such systems do not exist, then the Fermi level of any intermetallic material is constrained to fall on a predictable side of the hybridization gap region. This then leads to definite predictions for the signs of the thermopower and Hall effect, as discussed in Sec. VIF.

In the Kondo regime of the one-parameter version, for a single impurity, we have just seen that removal of \mathcal{E}_σ^- eliminates *all* of the interaction energy $\langle H \rangle_{\text{int}}$. It is therefore clear that (minus) the expression (30) is just the energy required to “unquench” the magnetic moment at

$T=0$. (This same expression is obtained for the case of a single impurity.) This provides a very reasonable definition for the Kondo temperature,¹⁰⁵ and therefore this lends some support for the definition (57) for T_f . More generally for lattice systems, however, $\rho(\epsilon_F)^{-1}$ cannot be identified with $|N^{-1}\langle H \rangle_{\text{int}}|$, nor can either of these be identified with a relevant average over the \mathcal{E}_k^- spectrum. Thus, if we define a “Kondo temperature” for lattice systems in terms of a suitable average spin-unquenching energy, to characterize the “Kondo crossover” of Sec. VIE, this T_K will generally differ from the T_f of (57), and the ratio T_K/T_f will be material dependent. Finally, we note that the “unquenching” energy \mathcal{E}_σ^- is reminiscent of the phenomenological E_{ex} parameter of Sales and Wohlleben.¹ It cannot be identical, however, because of these authors’ use of a renormalized temperature.

VII. CONCLUDING REMARKS

An explicit realization of the Luttinger picture of a periodic Fermi liquid has been presented. Since this feature is essentially guaranteed by the method of construction (initial state $|\Phi_c \Phi_f\rangle$ with sharp Fermi surface, and method of generating quasiparticles), two types of questions naturally arise. First, is the Luttinger picture really correct for the present (Anderson lattice) Hamiltonian, i.e., is the low-temperature behavior really that of a Fermi liquid? Second, are the detailed results quantitatively or even qualitatively reliable?

Because the first question can only be answered definitively by an exact solution,⁸ our need to *assume* a Fermi-liquid phase is shared by most of the other theoretical literature on Fermi liquids. A more realistic goal is to compare the free energies of this and the likely competing phases, namely the magnetic and the superconducting phases. More work in this direction is needed.

Concerning the validity of the detailed results, we are again faced with the lack of any exact results to compare with. There are, however, a number of comparisons that appear to be significant. Experimental phenomenology,¹⁻³ high-temperature perturbation theory,⁹⁸ and Ward-identity studies⁹⁹ all suggest close connections between the single-impurity and lattice cases. We do indeed find a number of close formal correspondences with the very significant body of $(1/N_f)$ -expansion and Bethe-ansatz results (Sec. VIF). There is also a reasonably good overall consistency with experimental phenomenology (Secs. VIB–VIE). In particular, a number of low-temperature features of normal heavy-fermion materials have been interpreted for the first time.

Several different weightings of the quasiparticle state density have been considered here: (a) The total quasiparticle state density,

$$\rho(E) = d(\text{number of quasiparticle states})/dE .$$

This is the quantity relevant for low-temperature thermodynamic properties, such as specific heat and magnetic susceptibility. (b) The “spectral” conduction-electron and f -electron state densities, $\rho_c(E)$ and $\rho_f(E)$. These are obtained by weighting each quasiparticle by an appropriate transition probability describing the sudden addition or

removal of a "bare" conduction or f electron. For the one-parameter version the conduction-state transition probabilities \mathcal{W}_{ck}^\pm are the same as the conduction-state probabilities P_{ck}^\pm , calculated in the obvious hybridization-model manner, but the f transition probabilities \mathcal{W}_{fk}^\pm are smaller than the f probabilities P_{fk}^\pm by a factor $1-\xi$. For this reason, $\rho_c(E)+\rho_f(E) < \rho(E)$. These spectral densities are relevant for the high-energy electron spectroscopies [XPS, ultraviolet photoemission spectroscopy (UPS), and BIS]. (This f spectral intensity must, however, be supplemented by an important nonquasiparticle contribution.) Also, ρ_c applies to relaxation via excitation of quasiparticles, in electron spin resonance and ultrasonic attenuation, while in nuclear magnetic resonance there is also a contribution from $(1-\xi)^{-1}\rho_f$. (c) The quantity $\bar{\sigma}(E)$, which relates to electrical conductivity, has a character quite opposite to that of $\rho(E)$. Instead of having sharp peaks near the hybridization gap edges, it is strongly suppressed near the gap. (d) Inelastic neutron scattering involves f -electron probabilities P_{fk}^\pm , but not the "sudden" factors $(1-\xi)$ found in the \mathcal{W}_{fk}^\pm 's. The qualitative features of these different density functions enable one to readily understand a number of basic features of VF phenomenology. Also, some of the more-detailed low-temperature phenomenology can now be explained, or at least rationalized.

A significant feature of the present approach is that *all* aspects of the quasiparticles (such as the width and position of " f -resonance" structure, and the Fermi level) are fully determined, once the details of the Hamiltonian and the number of electrons per site are specified. On the other hand, a very important aspect lies outside the scope of this work: the position of ε_f with respect to the conduction band. This is merely an input parameter here. In reality, this parameter is determined by a variety of phenomenological considerations, which have been explored in much detail by Wohlleben and co-workers.¹⁰⁶ The present type of Hamiltonian also has some potentially serious physical omissions: the Coulomb interaction U_{fd} between f and conduction electrons, electron-phonon coupling, intrinsic f -band dispersion, and a noninfinite f - f Coulomb interaction U .

There are, of course, approximations in this treatment. Comparison with $(1/N_f)$ -expansion results suggests that the level of sophistication in our two-parameter model should be adequate for most purposes. A potentially more serious approximation is our neglect of the site-exclusion problem. This will probably have to be refined before this work can be extended to arbitrary finite U . A particularly important problem concerns the treatment of a *finite* density of \mathcal{S}^- quasiparticles. Improvement here will be essential for higher-temperature studies, namely, for $T \gtrsim T_f$. Also, a number of the expected consequences of quasiparticle interactions have been ignored.

ACKNOWLEDGMENTS

I am indebted to many people for helpful discussions. Among experimentalists, discussions with Z. Fisk, J. L. Smith, F. Steglich, G. R. Stewart, J. D. Thompson, and D. Wohlleben have been particularly stimulating for this

work. Beth-ansatz and $(1/N_f)$ -expansion investigators, especially O. Gunnarsson, A. C. Hewson, Y. Kuramoto, J. W. Rasul, N. Read, and P. Schlottmann, have provided much helpful instruction. I am grateful to A. Hewson for providing unpublished Beth-ansatz results for the Wilson ratio. The main impetus for this work was the observation of R. M. Martin and J. W. Allen that the Luttinger picture of a periodic Fermi liquid is the correct low-temperature description for VF materials. This work is supported by the U.S. Department of Energy.

APPENDIX

Formulas concerning the parameter μ are presented here. This parameter is first encountered in connection with the optimization of A_k , Eq. (24). We therefore define

$$\mathcal{A} = -\frac{1}{N} \frac{\partial \langle H \rangle}{\partial \mathcal{D}} = \frac{1}{N} \sum_{k, \sigma} \frac{\varepsilon_k A_k^2 + 2V_k A_k}{(\mathcal{D} + A_k^2)^2}. \quad (\text{A1})$$

Now consider the increment $\delta \mathcal{D}$ arising from a variation δA_k . According to Eq. (22),

$$\delta \mathcal{D} = \frac{\delta \mathcal{D}}{N} \sum_{k', \sigma} \left[\frac{A_{k'}^2}{\mathcal{D} + A_{k'}^2} \right]^2 + \frac{4A_k \delta A_k}{N} \left[\frac{\mathcal{D}}{\mathcal{D} + A_k^2} \right]^2, \quad (\text{A2})$$

therefore

$$\frac{\delta \mathcal{D}}{\delta A_k} = \frac{4A_k}{N \mathcal{B}} \left[\frac{\mathcal{D}}{\mathcal{D} + A_k^2} \right]^2, \quad (\text{A3})$$

where

$$\mathcal{B} = 1 - \frac{1}{N} \sum_{k, \sigma} \left[\frac{A_k^2}{\mathcal{D} + A_k^2} \right]^2. \quad (\text{A4})$$

Comparison with Eq. (24) shows that

$$\mu = \mathcal{A} \mathcal{D} / \mathcal{B}. \quad (\text{A5})$$

The optimization condition (24) can now be used to simplify this expression for μ . We note, from (24), that

$$\begin{aligned} \varepsilon_k A_k^2 + 2V_k A_k &= V_k A_k \{ [(\varepsilon_k - \mu) A_k / V_k + 2] + \mu A_k / V_k \} \\ &= (V_k A_k / \mathcal{D})(\mathcal{D} + A_k^2) + \mu A_k^2. \end{aligned} \quad (\text{A6})$$

Inserting this in (A1) and (A5), we find

$$\begin{aligned} \mu &= \mathcal{B}^{-1} \left[\frac{1}{N} \sum_{k, \sigma} \frac{V_k A_k}{\mathcal{D} + A_k^2} + \frac{\mu}{N} \sum_{k, \sigma} \frac{\mathcal{D} A_k^2}{(\mathcal{D} + A_k^2)^2} \right] \\ &\equiv \mathcal{B}^{-1} \{ \mathcal{F} + \mu \mathcal{G} \} = \mathcal{F} / (\mathcal{B} - \mathcal{G}) \\ &= \frac{\mathcal{D}}{N} \sum_{k, \sigma} \frac{V_k A_k}{\mathcal{D} + A_k^2}. \end{aligned} \quad (\text{A7})$$

The last of these steps follows from (18), i.e.,

$$\mathcal{B} - \mathcal{G} = 1 - \frac{1}{N} \sum_{k, \sigma} \frac{A_k^2}{\mathcal{D} + A_k^2} = \mathcal{D}^{-1}. \quad (\text{A8})$$

This result for μ was used in Eq. (28). Equation (A6) can also be used to transform the expression (17) for $\langle H \rangle$, thus

$$\langle H \rangle = \sum_{k, \sigma} \epsilon_k + \mathcal{D}^{-1} \sum_{k, \sigma} V_k A_k + N \mu \xi. \quad (\text{A9})$$

This was used in obtained Eq. (29).

In obtaining the quasiparticle expression (35), we have used (22) to find

$$\begin{aligned} \langle H \rangle &= \sum_{k, \sigma} \epsilon_k + \sum_{k, \sigma} (\epsilon_k A_k^2 + 2V_k A_k) \frac{P_2^0}{\mathcal{D}} \left[1 + \left[-\frac{A_k^2 P_2^0}{\mathcal{D}} \right] + \left[-\frac{A_k^2 P_2^0}{\mathcal{D}} \right]^2 + \dots \right] \\ &= \sum_{k, \sigma} \epsilon_k + \sum_{k, \sigma} \frac{\epsilon_k A_k^2 + 2V_k A_k}{(\mathcal{D}/P_2^0) + A_k^2}, \end{aligned} \quad (\text{A12})$$

and (18) must be replaced by

$$\begin{aligned} \mathcal{D} &= 1 + \frac{1}{N} \sum_{k, \sigma} A_k^2 \left[1 + \left[-\frac{A_k^2 P_2^0}{\mathcal{D}} \right] + \left[-\frac{A_k^2 P_2^0}{\mathcal{D}} \right]^2 + \dots \right] \\ &= 1 + \frac{1}{N} \sum_{k, \sigma} \frac{A_k^2 (\mathcal{D}/P_2^0)}{(\mathcal{D}/P_2^0) + A_k^2}. \end{aligned} \quad (\text{A13})$$

These geometric-series forms follow naturally from the diagrammatic analysis, as will be shown in a future publication. A crucial point, here, is to note that the A_k^2 factor in front of the series in (A13) is *not* accompanied by a P_2^0 factor. This is best justified diagrammatically, but the reason can be understood by considering a single-impurity system, in which case the geometric-series factors (within large square brackets) in (A12) and (A13) are absent. It is then clear that only the P_2^0 factor remaining in (A12) is needed; inclusion of a similar factor in (A13) would amount to double counting.

We now consider the changes in \mathcal{D} and $\langle H \rangle$ which result from $\delta P_2^0 = -(1/N)$. Using

$$\delta \left(\frac{\mathcal{D}}{P_2^0} \right) = \frac{\delta \mathcal{D}}{P_2^0} - \frac{\mathcal{D}}{(P_2^0)^2} \delta P_2^0 \approx \delta \mathcal{D} + \frac{\mathcal{D}}{N}, \quad (\text{A14})$$

the variation of (A13) gives

$$\delta \mathcal{D} = -\frac{1}{N \mathcal{B}} \left[\frac{A_k^2}{\mathcal{D} + A_k^2} \right]. \quad (\text{A10})$$

The simplified expression (36) then follows from (A6).

The uniform shift of the \mathcal{E}^- quasiparticle energies (38), by the amount μ , is the result of a more subtle analysis. When $f k \uparrow$ is removed from Φ_f , the "initial" f^2 occupation probability at each site becomes less than unity,

$$P_2^0 = P^0(f^2) = 1 - \frac{1}{N}. \quad (\text{A11})$$

The effect of each virtual transition $j\sigma \rightarrow k'\sigma$ is thereby reduced by this probability P_2^0 . We find that (17) must be replaced by

$$\begin{aligned} \delta \mathcal{D} &= \frac{1}{N} \sum_{k, \sigma} \left[\frac{A_k^2}{(\mathcal{D}/P_2^0) + A_k^2} \right]^2 \delta \left(\frac{\mathcal{D}}{P_2^0} \right) \\ &= (1 - \mathcal{B})(\delta \mathcal{D} + \mathcal{D}/N), \end{aligned} \quad (\text{A15})$$

whereby

$$\delta \mathcal{D} = (1 - \mathcal{B}) \mathcal{D} / N \mathcal{B}. \quad (\text{A16})$$

The net change in $\langle H \rangle$ due to δP_2^0 is therefore

$$\frac{\partial \langle H \rangle}{\partial (\mathcal{D}/P_2^0)} \left[\frac{\mathcal{D}}{N} + \frac{(1 - \mathcal{B}) \mathcal{D}}{N \mathcal{B}} \right] = -N \mathcal{A} \left[\frac{\mathcal{D}}{N \mathcal{B}} \right] = -\mu. \quad (\text{A17})$$

This energy change has come from the *removal* of a quasiparticle. The corresponding term in the quasiparticle energy must therefore have the opposite sign, hence the term μ in Eq. (38).

¹B. C. Sales and D. K. Wohlleben, Phys. Rev. Lett. 35, 1240 (1975); B. C. Sales, J. Low Temp. Phys. 28, 107 (1977).

²D. M. Newns and A. C. Hewson, J. Phys. F 10, 2429 (1980). See also, E. E. Havinga, K. H. J. Buschow, and H. J. Van Daal, Solid State Commun. 13, 621 (1973).

³D. M. Newns, A. C. Hewson, J. W. Rasul, and N. Read, J. Appl. Phys. 53, 7877 (1982). See also, Y. Kuramoto and E. Müller-Hartmann, in *Valence Fluctuations in Solids*, edited by L. M. Falicov, W. Hanke, and M. P. Maple (North-Holland,

Amsterdam, 1981), p. 139.

⁴B. Batlogg, P. H. Schmidt, and J. M. Rowell, in *Valence Fluctuations in Solids*, Ref. 3, p. 267.

⁵T. Kasuya, K. Takegahara, T. Fujita, T. Tanaka, and E. Bannai, J. Phys. (Paris) Colloq. 40, C5-308; J. W. Allen, B. Batlogg, and P. Wachter, Phys. Rev. B 20, 4807 (1979); S. von Molnar, T. Theis, A. Benoit, A. Briggs, J. Flouquet, J. Ravex, and Z. Fisk, in *Valence Instabilities*, edited by P. Wachter and H. Boppart (North-Holland, Amsterdam, 1982), p. 389.

- 6P. Haen, F. Lapierre, J. M. Mignot, R. Tournier, and F. Holtzberg, *Phys. Rev. Lett.* **43**, 304 (1979).
- 7G. W. Crabtree, W. R. Johanson, A. S. Edelstein, and O. D. McMasters, in *Valence Fluctuations in Solids*, Ref. 3, p. 93.
- 8J. M. Luttinger, *Phys. Rev.* **119**, 1153 (1960).
- 9L. D. Landau, *Zh. Eksp. Teor. Fiz.* **30**, 1058 (1956) [*Sov. Phys.—JETP* **3**, 920 (1957)].
- 10These features are all contained, at least implicitly, in the original works of L. D. Landau (Ref. 9) and A. A. Migdal (*Zh. Eksp. Teor. Fiz.* **32**, 399 (1957) [*Soviet Phys.—JETP* **5**, 333 (1957)]), but J. M. Luttinger has presented a particularly clear and systematic analysis.
- 11R. M. Martin and J. W. Allen, *J. Appl. Phys.* **50**, 7561 (1979), in *Valence Fluctuations in Solids*, Ref. 3, p. 85; R. M. Martin, *Phys. Rev. Lett.* **48**, 362 (1982).
- 12H. R. Krishna-murthy, K. G. Wilson, and J. W. Wilkins, *Phys. Rev. Lett.* **35**, 1101 (1975); H. R. Krishna-murthy, J. W. Wilkins, and K. G. Wilson, *Phys. Rev. B* **21**, 1003 (1980); **21**, 1044 (1980).
- 13A. M. Tsvetick and P. B. Wiegmann, *Adv. Phys.* **32**, 453 (1983), and references therein; *Z. Phys. B* **54**, 201 (1984); A. M. Tsvetick, *J. Phys. C* **18**, 159 (1985).
- 14N. Andrei, K. Furuya, and J. H. Lowenstein, *Rev. Mod. Phys.* **55**, 331 (1983), and references therein; V. T. Rajan, *Phys. Rev. Lett.* **51**, 308 (1983); A. Okiji and N. Kawakami, *ibid.* **50**, 1157 (1983), *J. Appl. Phys.* **55**, 1931 (1984).
- 15A. C. Hewson and J. W. Rasul, *J. Phys. C* **16**, 6799 (1983); J. W. Rasul and A. C. Hewson, *J. Phys. C* **17**, 2555 (1984); **17**, 3337 (1984).
- 16P. Schlottmann, *Z. Phys. B* **51**, 49 (1983); **56**, 127 (1984); **57**, 23 (1984); *J. Phys. C* **17**, L267 (1984); *Phys. Lett.* **100A**, 509 (1984); *J. Magn. Magn. Mater.* **47-48**, 367 (1985).
- 17T. V. Ramakrishnan, in *Valence Fluctuations in Solids*, Ref. 3, p. 13; T. V. Ramakrishnan and K. Sur, *Phys. Rev. B* **26**, 1798 (1982).
- 18O. Gunnarsson and K. Schönhammer, *Phys. Rev. Lett.* **50**, 604 (1983); *Phys. Rev. B* **28**, 4315 (1983).
- 19F. C. Zhang and T.-K. Lee, *Phys. Rev. B* **28**, 33 (1983).
- 20P. Coleman, *Phys. Rev. B* **29**, 3035 (1984).
- 21N. Read and D. M. Newns, *J. Phys. C* **16**, 3273 (1983); **16**, L1055 (1983).
- 22N. Read, *J. Phys. C* **18**, 2651 (1985); N. Read and D. M. Newns, *Solid State Commun.* **52**, 993 (1984).
- 23J. W. Rasul and A. C. Hewson, *J. Phys. C* **17**, 2555 (1984); **17**, 3337 (1984).
- 24P. Schlottmann, *Phys. Lett.* **100A**, 509 (1984).
- 25P. Coleman, *Phys. Rev. B* **28**, 5255 (1983). See also, P. Coleman, *Phys. Rev. B* **29**, 3035 (1984).
- 26J. W. Rasul, N. Read, and A. C. Hewson, *J. Phys. C* **16**, L1079 (1983).
- 27(a) N. Read, D. M. Newns, and S. Doniach, *Phys. Rev. B* **30**, 3841 (1984); (b) N. Read and D. M. Newns, *Solid State Commun.* **52**, 993 (1984).
- 28G. Czycholl, *Phys. Rev. B* **31**, 2867 (1985).
- 29Essentially all previous $(1/N_f)$ -expansion studies of the lattice problem (Refs. 25–28) have concluded that the sites become completely uncoupled in the limit $N_f \rightarrow \infty$. (References 25 and 28 emphasize, however, that there would still be an important mutual influence due to the self-consistent chemical potential.) We disagree, and we attribute this false conclusion either to unrealistic assumptions about the hybridization matrix elements V_{km} (a point emphasized in Ref. 28), or to incorrect analysis of these V_{km} 's. For example, in Refs. 26 and 27 it is argued that for the two-site term a suitable choice of quantization axis leads to a factor $\delta_{mm'}$, which thereby eliminates a factor of N_f . This overlooks the fact that the normalization of the spherical harmonics Y_l^m (page 1081 of Ref. 26) contributes a compensating factor of $(2l+1)=N_f$. Our studies of this issue also assume V_{km} proportional to Y_l^m . We sum the m 's first, using $4\pi \sum_m Y_l^m(\hat{\mathbf{k}}') Y_l^m(\hat{\mathbf{k}}) = (2l+1)P_l(\hat{\mathbf{k}} \cdot \hat{\mathbf{k}}')$, and then obtain $\delta_{kk'}$ from site summation, leaving explicit factors of $(2l+1)$. We thereby find that the multisite terms are all of relative order N_f^0 . These multisite terms are then summed as geometric series, as indicated in Eqs. (A12) and (A13) of the Appendix.
- 30Hubbard I approximation: (a) C. M. Varma and Y. Yafet, *Phys. Rev. B* **13**, 2950 (1976); (b) B. H. Brandow, *Int. J. Quantum Chem. Symp.* **13**, 423 (1979); (c) M. Roberts and K. W. H. Stevens, *J. Phys. C* **13**, 5941 (1980); D. L. Huber, *Phys. Rev. B* **28**, 860 (1983); **29**, 456 (1984), *J. Appl. Phys.* **55**, 1928 (1984); M. Matlack and W. Nolting, *Z. Phys. B* **55**, 103 (1984). See also, D. A. Smith, *J. Phys. C* **1**, 1263 (1968); R. Kishore and S. K. Joshi, *Phys. Rev. B* **2**, 1411 (1970).
- 31Modified Hubbard I approximation: A. J. Fedro and S. K. Sinha, in *Valence Fluctuations in Solids*, Ref. 3, p. 329; T.-K. Lee, *ibid.*, p. 405.
- 32Coherent-potential approximation (CPA) or alloy-analogy approximation: S. K. Chatak, M. Avignon, and K. H. Bennemann, *J. Phys. F* **6**, 1441 (1976); O. Sakai, S. Seki, and M. Tachiki, *J. Phys. Soc. Jpn.* **45**, 1465 (1978); R. M. Martin and J. W. Allen, *J. Appl. Phys.* **50**, 7561 (1979); H. J. Leder and G. Czycholl, *Z. Phys. B* **35**, 7 (1979); **38**, 219 (1980); G. Czycholl and H. J. Leder, *ibid.* **44**, 59 (1981); **48**, 67 (1982).
- 33Hubbard III approximation: (a) B. H. Brandow, in *Valence Instabilities*, Ref. 5, p. 37; (b) H. G. Baumgartel and E. Müller-Hartmann, *ibid.*, p. 57; G. Czycholl, *Phys. Rev. B* **31**, 2867 (1985).
- 34Crossing-symmetric decoupling: K. Hoshino and Y. Kurata, *J. Phys. F* **9**, 131 (1979); Y. Kurata, *ibid.* **10**, 893 (1980).
- 35Diagram summation: N. Grewe and H. Keiter, *Phys. Rev. B* **24**, 4420 (1981); N. Grewe, *Z. Phys. B* **52**, 193 (1983); *Solid State Commun.* **50**, 19 (1984); Y. Kuramoto and C. Horie, *J. Magn. Magn. Mater.* **47-48**, 343 (1985). See also, Ref. 33(a), and H. Keiter and G. Morandi, *Phys. Rep.* **109**, 227 (1984).
- 36Single-impurity ansatz for self-energy: A. Yoshimori and H. Kasai, *J. Magn. Magn. Mater.* **31-34**, 475 (1983); F. J. Ohkawa, *J. Phys. Soc. Jpn.* **52**, 3886 (1983); M. Tachiki and S. Maekawa, *Phys. Rev. B* **29**, 2497 (1984); G. Czycholl and S. Doniach, *J. Magn. Magn. Mater.* **47-48**, 17 (1985); N. Grewe and T. Pruschke, *Z. Phys. B* **60**, 311 (1985).
- 37Phenomenological self-energy: H. Razafimandimby, P. Fulde, and J. Keller, *Z. Phys. B* **54**, 111 (1984); N. Grewe, *ibid.* **56**, 111 (1984); N. d'Ambrumenil and P. Fulde, *J. Magn. Magn. Mater.* **47-48**, 1 (1985).
- 38C. Lacroix and M. Cyrot, *Phys. Rev. B* **20**, 1969 (1979); M. Lavagna, C. Lacroix, and M. Cyrot, *J. Phys. F* **12**, 745 (1982), *Phys. Lett.* **89A**, 154 (1982); **90A**, 210 (1982).
- 39P. Coleman, *J. Magn. Magn. Mater.* **47-48**, 323 (1985); in *Theory of Heavy Fermions and Valence Fluctuations*, Springer Series in Solid State Science 62 edited by T. Kasuya and T. Saso (Springer, Berlin, 1985), p. 163.
- 40R. Jullien, J. Fields, and S. Doniach, *Phys. Rev. Lett.* **38**, 1500 (1977); *Phys. Rev. B* **16**, 4889 (1977).
- 41R. Jullien, P. Pfeuty, J. N. Fields, and S. Doniach, *J. Phys. (Paris) Colloq.* **40**, C5-293 (1979); R. Jullien, P. Pfeuty, A. K. Bhattacharjee, and B. Coqblin, *J. Appl. Phys.* **50**, 7555 (1979); L. C. Lopes, R. Jullien, A. K. Bhattacharjee, and B. Coqblin,

- in *Valence Fluctuations in Solids*, Ref. 3, p. 383; Phys. Rev. B **26**, 2640 (1982).
- ⁴²R. Jullien and R. M. Martin, J. Appl. Phys. **53**, 2137 (1982); Phys. Rev. B **26**, 6173 (1982); R. Jullien, in *Valence Instabilities*, Ref. 5, p. 11.
- ⁴³K. Yamada and K. Yosida, J. Magn. Mater. **31-34**, 461 (1983); H. Kaga and Y. Shibuya, *ibid.*, **31-34**, 455 (1983). See also, Ref. 99.
- ⁴⁴K. W. H. Stevens, J. Phys. C **11**, 985 (1978); R. G. Arnold and K. W. H. Stevens *ibid.* **12**, 5037 (1979); K. W. H. Stevens and R. G. Arnold, *ibid.* **12**, 5051 (1979).
- ⁴⁵B. H. Brandow, in *Crystalline Electric Field and Structural Effects in f-Electron Systems*, edited by J. E. Crow, R. P. Guertin, and T. W. Mihalisin (Plenum, New York, 1980), p. 353; in *Valence Fluctuations in Solids*, Ref. 3, p. 357.
- ⁴⁶P. Fazekas, Z. Phys. B **47**, 301 (1982); **53**, 197 (1983); J. Magn. Mater. **47-48**, 375 (1985). This work applies the Gutzwiller variational method in a systematic manner. There is also an intuitive application of Gutzwiller's results for the Hubbard Hamiltonian: T. M. Rice, K. Ueda, H. R. Ott, and H. Rudigier, Phys. Rev. B **31**, 594 (1985); T. M. Rice and K. Ueda, in *Theory of Heavy Fermions and Valence Fluctuations*, Ref. 39, p. 216; Phys. Rev. Lett. **55**, 995 (1985).
- ⁴⁷N. Fuchikami and S. Ishioka, J. Phys. C **18**, 319 (1985).
- ⁴⁸The simplest approximation, namely Hartree-Fock [H. J. Leder and B. Mühlischlegel, Z. Phys. B **29**, 341 (1978)], does account for both of these aspects, but in actual materials U is much too strong for this approximation to be valid.
- ⁴⁹There is, however, much similarity between our present results and the low-temperature results obtained by functional integration in Refs. 27, 38, and 39. The same renormalization of V_k , Eq. (40), is obtained in Refs. 27(b) and 39. An ϵ_f renormalization similar to Eq. (39) is also obtained in these works, but is not identical because of the problem discussed in Ref. 29. Our result for the ϵ_f renormalization was, however, obtained in Ref. 31.
- ⁵⁰S. H. Liu, P. Burgardt, K. A. Gschneidner, Jr., and S. Legvold, J. Phys. F **6**, L55 (1976); S. Doniach, Physica **91B**, 231 (1977); C. D. Bredl, F. Steglich, and K. D. Schotte, Z. Phys. B **29**, 327 (1978); F. Steglich, C. D. Bredl, M. Loewenhaupt, and K. D. Schotte, J. Phys. (Paris) Colloq. **40**, C5-301 (1979); A. Benoit, J. Flouquet, M. Ribault, F. Flouquet, G. Chouteau, and R. Tournier, J. Phys. (Paris) Lett. **39**, L94 (1978); A. Benoit, J. Flouquet, and M. Ribault, J. Phys. (Paris) Colloq. **40**, C5-328 (1979); B. Barbara, M. Cyrot, C. Lacroix-Lyon-Caen, and M. F. Rossignol, *ibid.* **40**, C5-340 (1979); A. M. Tselvick, Zh. Eksp. Teor. Fiz. **76**, 2260 (1979) [Sov. Phys.—JETP **49**, 1142 (1979)]; A. F. Barabanov and A. M. Tselvick, Fiz. Tverd. Tela (Leningrad) **21**, 3214 (1979) [Sov. Phys.—Solid State **21**, 1855 (1979)]; C. Proetto and A. Lopez, Phys. Rev. B **25**, 7037 (1982); D. Gignoux and J. C. Gomez-Sal, *ibid.* **30**, 3967 (1984).
- ⁵¹B. H. Brandow, Rev. Mod. Phys. **39**, 771 (1967).
- ⁵²B. H. Brandow, Int. J. Quantum Chem. **15**, 207 (1979).
- ⁵³It has, however, been demonstrated that this formalism is well suited for concentrated local-moment systems: B. H. Brandow, Adv. Phys. **26**, 651 (1977).
- ⁵⁴B. H. Brandow, J. Magn. Mater. **47-48**, 372 (1985).
- ⁵⁵This Ψ is a generalization, to intermetallic systems, of the lattice variational Ψ introduced by Stevens, Ref. 44; it differs from the form used in Refs. 30(b) and 45 by the presence of the conduction electrons in Φ_c . Note that $|\Phi_c \Phi_f\rangle$ is not the ground state of the $V=0$ system, except in the perturbative regime.
- ⁵⁶Complete site equivalence (homogeneous mixed valence) has been confirmed experimentally, for a number of VF compounds, by a Mössbauer isomer shift spectrum consisting of just a single line, and by the absence of any crystallographic distortion at very low temperature.
- ⁵⁷P. Nozières, J. Low Temp. Phys. **17**, 31 (1974); P. Nozières and A. Blandin, J. Phys. (Paris) **41**, 193 (1980); K. Yamada, Prog. Theor. Phys. **53**, 970 (1975).
- ⁵⁸According to Green's-function theory, the true total $fk\sigma$ intensity must be unity. We expect the missing intensity, of strength ξ , to be shared between the regions $E \approx \epsilon_f$ and $E \approx -U$. The intensity of the latter region is presumably $\xi/2$, the true ground-state probability of a $j\sigma$ hole, leaving $\xi/2$ for the expected ϵ_f -peak intensity.
- ⁵⁹C. Lacroix, J. Phys. F **11**, 2389 (1981); J. Appl. Phys. **53**, 2131 (1982); O. Gunnarsson and K. Schönhammer, Phys. Rev. Lett. **50**, 604 (1983); Phys. Rev. B **28**, 4315 (1983); N. Grewe, Z. Phys. B **53**, 271 (1983); P. Coleman, Phys. Rev. B **29**, 3035 (1984); T. K. Lee and F. C. Zhang, J. Appl. Phys. **55**, 1936 (1984); F. C. Zhang and T. K. Lee, Phys. Rev. B **30**, 1556 (1984); Y. Kuramoto, Z. Phys. B **53**, 37 (1983); H. Kojima, Y. Kuramoto, and M. Tachiki, *ibid.* **54**, 293 (1984); Y. Kuramoto and H. Kojima, *ibid.* **57**, 95 (1984); J. Magn. Mater. **47-48**, 329 (1985); G. Czycholl, Phys. Rev. B **31**, 2867 (1985); N. E. Bickers, D. L. Cox, and J. W. Wilkins, J. Magn. Mater. **47-48**, 335 (1985); Phys. Rev. Lett. **54**, 230 (1985).
- ⁶⁰See, for example, L. I. Johansson, J. W. Allen, T. Gustafsson, I. Lindau, and S. B. M. Hagstrom, Solid State Commun. **28**, 53 (1978); R. D. Parks, N. Mårtensson, and B. Reihl, in *Valence Instabilities*, Ref. 5, p. 239; Y. Baer, H. R. Ott, J. C. Fuggle, and L. E. DeLong, Phys. Rev. B **24**, 5384 (1981); A. Franciosi, J. H. Weaver, N. Mårtensson, and M. Croft, *ibid.* **24**, 3651 (1981); J. W. Allen, S.-J. Oh, I. Lindau, M. B. Maple, J. F. Suassuna, S. B. Hagström, *ibid.* **26**, 445 (1982); J. C. Fuggle, F. U. Hillebrecht, Z. Zolnieriek, R. Lässer, C. Freiburg, O. Gunnarsson, and K. Schönhammer, *ibid.* **27**, 7330 (1983); R. D. Parks, S. Raaen, M. L. den Boer, Y.-S. Chang, and G. P. Williams, Phys. Rev. Lett. **52**, 2176 (1984); J. Magn. Mater. **47-48**, 163 (1985).
- ⁶¹D. D. Koelling, Solid State Commun. **43**, 247 (1982); P. Strange and D. M. Newns, J. Phys. C (to be published).
- ⁶²O. Gunnarsson and K. Schönhammer, J. Magn. Mater. **47-48**, 266 (1985); Phys. Rev. B **31**, 4815 (1985).
- ⁶³S. H. Liu and K. M. Ho, Phys. Rev. B **26**, 7052 (1982); **28**, 4220 (1983); **30**, 3039 (1984); M. D. Nunez-Regueiro and M. Avignon, Phys. Rev. Lett. **55**, 615 (1985); M. Takeshige, O. Sakai, and T. Kasuya, in *Theory of Heavy Fermions and Valence Fluctuations*, Ref. 39, p. 120.
- ⁶⁴B. H. Brandow, J. Magn. Mater. **52**, 25 (1985).
- ⁶⁵K. Yosida and A. Sakurai, J. Magn. Mater. **15-18**, 949 (1980); O. Gunnarsson and K. Schönhammer, Phys. Rev. B **28**, 4315 (1983); J. W. Rasul and A. C. Hewson, J. Phys. C **16**, L933 (1983).
- ⁶⁶See Newns *et al.*, Ref. 3. In a similar study of Ce compounds (T. Mihalisin, P. Scoboria, and J. A. Ward, in *Valence Fluctuations in Solids*, Ref. 3, p. 61) the singular behavior as $\xi \rightarrow 1$ was not observed. We attribute this to the alloying aspect of the latter work, whereby substitutional disorder smears out the density-of-states peak and prevents the attainment of very large m^* values.
- ⁶⁷See, for example, J. Lawrence, Phys. Rev. B **20**, 3770 (1979); J. Lawrence and M. T. Béal-Monod, in *Valence Fluctuations in Solids*, Ref. 3, p. 53; N. E. Bickers, D. L. Cox, and J. W. Wilkins, J. Magn. Mater. **47-48**, 335 (1985); Phys. Rev.

- Lett. **54**, 230 (1985).
- ⁶⁸G. P. Meisner, A. L. Giorgi, A. C. Lawson, G. R. Stewart, J. O. Willis, M. S. Wire, and J. L. Smith, Phys. Rev. Lett. **53**, 1829 (1984).
- ⁶⁹G. R. Stewart, Rev. Mod. Phys. **56**, 755 (1984).
- ⁷⁰P. Scoboria, J. E. Crow, and T. Mihalisin, J. Appl. Phys. **50**, 1895 (1979). See also, S. Doniach, in *The Actinides: Electronic Structure and Related Properties, Vol. II*, edited by A. J. Freeman and J. B. Darby, Jr. (Academic, New York, 1974), especially pp. 63–67.
- ⁷¹K. Andres, J. E. Graebner, and H. R. Ott, Phys. Rev. Lett. **35**, 1779 (1975); J. Flouquet, J. C. Lasjaunias, and J. Peyrard, J. Appl. Phys. **53**, 2127 (1982); C. D. Bredl, S. Horn, F. Steglich, B. Luthi, and R. M. Martin, Phys. Rev. Lett. **52**, 1982 (1984); F. Steglich, C. D. Bredl, W. Lieke, U. Rauchschwalbe, and G. Sparn, Physica **126B**, 82 (1984); F. Steglich, U. Rauchschwalbe, U. Gottwick, H. M. Mayer, G. Sparn, N. Grewe, U. Poppe, and J. J. M. Franse, J. Appl. Phys. **57**, 3054 (1985); D. Jaccard and J. Flouquet, J. Magn. Magn. Mater. **47-48**, 45 (1985).
- ⁷²N. F. Mott, Philos. Mag. **30**, 403 (1974).
- ⁷³J. W. Allen, B. Batlogg, and P. Wachter, Phys. Rev. B **20**, 4807 (1979); T. Kasuya, M. Kasaya, K. Takegahara, T. Fujita, T. Goto, A. Tamaki, M. Takigawa, and H. Yasuoka, J. Magn. Magn. Mater. **31-34**, 447 (1983); G. Travaglini and P. Wachter, Phys. Rev. B **29**, 893 (1984); **30**, 5877 (1984); M. Kasaya, F. Iga, M. Takigawa, and T. Kasuya, J. Magn. Magn. Mater. **47-48**, 429 (1985).
- ⁷⁴B. H. Greer and S. M. Shapiro, in *Valence Fluctuations in Solids*, Ref. 3, p. 325; A. P. Murani, Phys. Rev. Lett. **54**, 1444 (1985); J. Magn. Magn. Mater. **47-48**, 142 (1985); R. M. Galeva, D. Givord, J. Pierre, A. P. Murani, J. Schweizer, C. Vetter, and K. R. A. Ziebeck, J. Magn. Magn. Mater. **52**, 103 (1985).
- ⁷⁵CeAl₃: A. S. Edelstein, C. J. Tranchita, O. D. McMasters, and K. A. Gschneidner, Jr., Solid State Commun. **15**, 81 (1974); J. Flouquet, J. C. Lasjaunias, and J. Peyrard, J. Appl. Phys. **53**, 2127 (1982); F. R. de Boer, J. Klaasse, J. Aarts, C. D. Bredl, W. Lieke, U. Rauchschwalbe, F. Steglich, R. Felten, U. Umhofer, and G. Weber, J. Magn. Magn. Mater. **47-48**, 60 (1985). CeCu₂Si₂: H. Schneider, Z. Kletowski, O. Oster, and D. Wohlleben, Solid State Commun. **48**, 1093 (1983). CeCu₆: T. Fujita, K. Satoh, Y. Onuki, and T. Komatsubara, J. Magn. Magn. Mater. **47-48**, 66 (1985).
- ⁷⁶Another possible explanation (which we have not studied numerically) is that the relevant conduction band might have *p*-like symmetry, and thus have $V_k \sim \cos(\pi k/k_{\max})$. Such a heavy-fermion material would then presumably have $k_F \sim \frac{1}{2}k_{\max}$, so that $|V_{kF}| \ll |V_k|_{\max}$ still holds. With multiple conduction bands, however, it is also possible that ϵ_F could fall in the pseudogap, just below the bottom of the \mathcal{E}^+ spike; this could also account for the large first peak.
- ⁷⁷A. A. Abrikosov, *Introduction to the Theory of Normal Metals*, Supplement 12 of *Solid State Physics*, edited by H. Ehrenreich, F. Seitz, and D. Turnbull (Academic, New York, 1972); see p. 44.
- ⁷⁸The arguments for a “minimal metallic conductivity” have generally assumed a normal conduction-band mass of order unity; see N. F. Mott, *Metal-Insulator Transitions* (Taylor and Francis, London, 1974). Because of the enormous m^* values in the present metallic materials, one might suppose that their resistivities could violate this bound. On the other hand, strong disorder scattering (of any type) should interfere with the correlations producing the large m^* , thus we believe that the resistivity should still be subject to such a bound, of order $1000 \mu\Omega \text{cm}$ (Mott’s estimate for a *d* conduction band). This is consistent with the data.
- ⁷⁹W. G. Baber, Proc. R. Soc. London **158**, 383 (1937); L. Colquitt, H. R. Fankhauser, and F. J. Blatt, Phys. Rev. B **4**, 292 (1971); C. Hodges, H. Smith, and J. W. Wilkins, *ibid.* **4**, 302 (1971).
- ⁸⁰K. Andres, J. E. Graebner, and H. R. Ott, Phys. Rev. Lett. **35**, 1779 (1975).
- ⁸¹K. H. J. Buschow, H. J. van Daal, F. E. Maranzana, and P. B. van Aken, Phys. Rev. B **3**, 1662 (1971); B. Cornut and B. Coqblin, *ibid.* **5**, 4541 (1972); Y. Lassailly, A. K. Bhattacharjee, and B. Coqblin, *ibid.* **31**, 7424 (1985). Crystal-field data for CeCu₂Si₂: S. Horn, E. Holland-Moritz, M. Loewenhaupt, F. Steglich, H. Scheuer, A. Benoit, and J. Flouquet, *ibid.* **23**, 3171 (1981). CeAl₃: A. P. Murani, K. Knorr, and K. H. J. Buschow, in *Crystal Field Effects in Metals and Alloys*, edited by A. Furrer (Plenum, New York, 1977), p. 268.
- ⁸²F. Steglich (private communication).
- ⁸³Y. Onuki, Y. Shimizu, and T. Komatsubara, J. Phys. Soc. Jpn. **53**, 1210 (1984); **54**, 304 (1985).
- ⁸⁴W. Felsch and K. Winzer, Solid State Commun. **13**, 569 (1973).
- ⁸⁵G. Remenyi, A. Briggs, J. Floquet, O. Laborde, and F. Lapiere, J. Magn. Magn. Mater. **31-34**, 407 (1983). The idea that magnetoresistance involves a competition or crossover between normal-metallic and Kondo behaviors was initially suggested by A. S. Edelstein, R. E. Majewski, and T. H. Blewett, in *Valence Instabilities and Related Narrow-Band Phenomena*, edited by R. D. Parks (Plenum, New York, 1977), p. 115.
- ⁸⁶U. Rauchschwalbe, W. Baus, S. Horn, H. Spille, F. Steglich, F. R. de Boer, J. Aarts, W. Assmus, and M. Herrmann, J. Magn. Magn. Mater. **47-48**, 33 (1985).
- ⁸⁷J. M. Ziman, *Electrons and Phonons* (Oxford University Press, London, 1960).
- ⁸⁸D. Jaccard and J. Sierro, in *Valence Instabilities*, Ref. 5, p. 409; E. Cattaneo, U. Hafner, and D. Wohlleben, *ibid.*, p. 451; F. Steglich, U. Rauchschwalbe, U. Gottwick, H. M. Mayer, G. Sparn, N. Grewe, U. Poppe, and J. J. M. Franse, J. Appl. Phys. **57**, 3054 (1985); A. Amato and J. Sierro, J. Magn. Magn. Mater. **47-48**, 526 (1985); E. Cattaneo, *ibid.* **47-48**, 529 (1985); D. Jaccard, J. M. Mignot, B. Bellarbi, A. Benoit, H. F. Braun, and J. Sierro, *ibid.* **47-48**, 23 (1985).
- ⁸⁹B. Wittershagen and D. Wohlleben, J. Magn. Magn. Mater. **47-48**, 497 (1985).
- ⁹⁰T. V. Ramakrishnan, P. Coleman, and P. W. Anderson, J. Magn. Magn. Mater. **47-48**, 498 (1985). See also, A. Fert, J. Phys. F **3**, 2126 (1973); A. Fert, A. Friedrich, and A. Hamzic, J. Magn. Magn. Mater. **24**, 231 (1981).
- ⁹¹J. M. Lawrence, J. D. Thompson, and Y. Y. Chen, Phys. Rev. Lett. **54**, 2537 (1985).
- ⁹²F. Steglich, C. D. Bredl, W. Lieke, U. Rauchschwalbe, and G. Sparn, Physica **126B**, 82 (1984); D. Jaccard and J. Flouquet, J. Magn. Magn. Mater. **47-48**, 45 (1985).
- ⁹³D. Jaccard and J. Flouquet, J. Magn. Magn. Mater. **47-48**, 45 (1985); R. Pott, R. Schefzyk, D. Wohlleben, and A. Junod, Z. Phys. B **44**, 17 (1981).
- ⁹⁴The present type of explanation was first employed by T. Gambke, B. Elschner, and L. L. Hirst, Phys. Rev. Lett. **40**, 1290 (1978); H. Schaeffer and B. Elschner, Z. Phys. B **53**, 109 (1983). See also F. Gandra, S. Schultz, S. B. Oseroff, Z. Fisk, and J. L. Smith (unpublished).
- ⁹⁵E. Bucher, B. Batlogg, D. J. Bishop, C. M. Varma, Z. Fisk,

- and J. L. Smith, *J. Appl. Phys.* **57**, 3060 (1985); B. Batlogg, D. Bishop, G. Golding, C. M. Varma, Z. Fisk, J. L. Smith, and H. R. Ott, *Phys. Rev. Lett.* **55**, 1319 (1985); B. Batlogg, D. Bishop, B. Golding, E. Bucher, J. Hufnagl, Z. Fisk, J. L. Smith, and H. R. Ott (unpublished).
- ⁹⁶D. E. MacLaughlin (private communication).
- ⁹⁷See, for example, J. D. Thompson and Z. Fisk, *Phys. Rev. B* **31**, 389 (1985).
- ⁹⁸T.-K. Lee and S. Chakravarty, *Phys. Rev. B* **22**, 3609 (1980), and references therein.
- ⁹⁹K. Yamada and K. Yosida, in *Theory of Heavy Fermions and Valence Fluctuations*, Ref. 39, p. 183. The same results had been found earlier, for the case $\xi < 1$, but unfortunately this was not adequately discussed: P. Schlottmann, *Phys. Rev. B* **24**, 5394 (1981), *J. Phys. C* **17**, L77 (1984); and private communication.
- ¹⁰⁰O. Gunnarsson and K. Schönhammer (private communication); *Phys. Rev. B* **31**, 4815 (1985).
- ¹⁰¹N. Grewe, *Z. Phys. B* **53**, 271 (1983); Y. Kuramoto and H. Kojima, *ibid.* **57**, 95 (1984); Müller-Hartman, *ibid.* **57**, 281 (1984).
- ¹⁰²A. C. Hewson (private communication).
- ¹⁰³In our previous studies [Refs. 30(b) and 45] we claimed that the resulting errors are only of order N^{-1} (N equals the number of sites, essentially infinite), but we now find that they are actually of order N^0 . This will be discussed elsewhere, when the diagrammatics is presented.
- ¹⁰⁴P. de Chatel, *Solid State Commun.* **41**, 853 (1982).
- ¹⁰⁵The “unquenching energy” is not one of the standard ways to define a characteristic temperature “ T_K ,” but this has appeared occasionally in phenomenological treatments. See, for example, E. E. Havinga, K. H. J. Buschow, and H. J. Van Daal, *Solid State Commun.* **13**, 621 (1973).
- ¹⁰⁶J. Röhler, D. Wohlleben, G. Kaindl, and H. Balster, *Phys. Rev. Lett.* **49**, 65 (1982); D. Wohlleben, in *Moment Formation in Solids*, edited by W. J. L. Buyers (Plenum, New York, 1984), p. 171; D. Wohlleben, in *Physics and Chemistry of Electrons and Ions in Condensed Matter*, edited by J. V. Acrivos, N. F. Mott, and A. D. Yoffe, NATO-ASI Series **130**, (Riedel, Dordrecht, 1984), p. 85; D. Wohlleben and J. Röhler, *J. Appl. Phys.* **55**, 1904 (1984); J. Röhler, D. Wohlleben, J. P. Kappler, and G. Krill, *Phys. Lett.* **103A**, 220 (1984); B. Wittershagen and D. Wohlleben, *J. Magn. Magn. Mater.* **47-48**, 79 (1985). See also, B. C. Sales and D. K. Wohlleben, *Phys. Rev. Lett.* **35**, 1240 (1975); B. C. Sales, *J. Low Temp. Phys.* **28**, 107 (1977).